THE ROLE OF STERICS AND ELECTRONICS ON NICKEL CATALYZED ISOMERIZATION OF ALLYLBENZENE

by

PARKER T. MORRIS

A THESIS

Presented to the Department of Chemistry
and the Robert D. Clark Honors College
in partial fulfillment of the requirements for the degree of
Bachelor of Science

May 2021

An Abstract of the Thesis of

Parker T. Morris for the degree of Bachelor of Science
in the Department of Chemistry to be taken June 2021

Title: The Role of Sterics and Electronics on Nickel Catalyzed Isomerization of Allylbenzene

Approved: *Amanda K. Cook, Ph.D.*
Primary Thesis Advisor

Alkenes are a ubiquitous chemical functional group that serve as starting materials for a variety of industrially relevant chemicals in the pharmaceutical, synthetic manufacturing, and fragrance industries. One way of controlling alkene positionality and geometry is through metal–catalyzed isomerization. Current academic research focuses heavily on precious metals such as platinum, ruthenium, and iridium which are expensive and have been seen to promote side reactivity. In this project, the earth abundant metal, nickel, is used as a cheap alternative to its more costly counterparts. Four nickel complexes have been synthesized and characterized by following and improving established literature protocols. The complexes were subjected to isomerization conditions with the model substrate allylbenzene to determine the role of sterics and electronics on overall yield, product distribution, E/Z ratio, and initial rate of reaction. No trends were seen with regards to product distribution, overall yield, or E/Z ratio. The initial rate of reaction, however, was seen to increase with respect to steric encumbrance, contrary to the proposed hypothesis that increasing sterics would decrease initial rate of reaction.

Acknowledgements

First and foremost, I need to thank Prof. Amanda Cook. Amanda has supported my career as a chemist and as an ethical scientist since the moment we met. After letting me begin work in her lab as a wildly underqualified sophomore, Amanda personally taught me the skills I would need to be successful in conducting real chemical research. She provided unflinching support over the last three years; acting not only as a mentor and teacher but as a pillar of encouragement and guidance as I looked towards my future in science. I am eternally grateful for the impact Amanda has had on my life both in and out of lab. I would be entirely remiss if I did not also give equal gratitude to Kiana Kawamura. Kiana was my graduate student mentor in the Cook lab and stood by my side for well over a year teaching me how to work in the lab safely and efficiently. Her unwavering patience with me as a student is something I will seek to emulate in all aspects of my life. Despite testing the limits of her patience on many occasions, she never gave up on me or my work. Both of these incredible scientists have molded my career in ways they may never know, and I will never be able to give them enough credit for their influence on my career and life.

I also need to thank all other members of the Cook lab. Alison Chang has helped me nearly as much as Kiana and Amanda, both reading my work and answering my never-ending stream of questions. Michael Hurst similarly is always available for procedural questions or guidance when the glovebox stops working or makes a funny noise. Over the last three years, I have always felt the support of the entire Cook lab and I am eternally grateful to all of them.

I also need to thank the members of my thesis committee, Prof. Michael Koscho, and Prof. Carol Paty. Dr. Koscho was my first introduction to organic chemistry and he has supported me behind the scenes over the course of my entire research career, writing countless letters of recommendation and now reading my thesis. In his organic chemistry teaching lab, I made my first imidazole compound and now, three years later, I am still making imidazoles. Prof. Carol Paty stepped up for me despite never having met before and I am so grateful for her selflessness and dedication to student success.

This project was directly funded by the Vice President for Research and Innovation Fellowship. I would like to specifically thank Karl Reasoner for his support with both the VPRI fellowship and my future career goals.

Finally, I must thank my parents, Chris Morris and Pam Triplett, and my brother, Josh Morris. I'm not sure any of them understand a word I say when I talk about my research, but they listen intently, nevertheless. I love you all.

Table of Contents

List of Figures

List of Tables

Introduction

Synthetic chemistry is vital to manufacturing daily household products such as perfumes, food additives, and synthetic materials.[1] Nearly every item we interact with daily is a product of some chemical synthesis. As such, the chemical industry manufactures a broad array of chemicals on the million tons scale yearly[1,2] and developing energy–efficient ways to create these materials is an important area of study for organic and inorganic chemists. One approach to increasing reaction efficiency is through the use of a metal catalyst.[1,2] Catalysts are used abundantly in industry because they make reactions faster and more selective, thus generating less waste. The fundamental goal of a catalyst is to reduce the energy barrier for a reaction. By reducing the reaction's energy barrier, the overall process generally requires lower temperatures, pressures, and/or reaction times. By eliminating costly reaction conditions, the process is greener, less expensive, and more efficient. Catalysts also help tune the product distribution in many synthetic reactions. Unfortunately, some of the most successful metal catalysts are derived from precious metals such as platinum, palladium, iridium, or ruthenium.[1,3] These metals are costly and mining processes to acquire them are detrimental to the environment.[1,3] As such, I am looking to use the earth abundant metal, nickel, as a more renewable, cheap alternative to precious metal catalysts.

Nickel has been used catalytically in academia for many years now with complexes such as Raney nickel seeing reactivity as early as the 1920's.[1,3] Since then, many nickel complexes have been used in a wide variety of reactions from isomerization to functionalization (the process of installing a functional group).[1,2,3] Despite its catalytic success, few studies have systematically probed the steric influence

of nickel complexes on catalytic reactivity and none have done so for isomerization reactions. Sterics, spatial area an organic ligand occupies, can be quantified using the parameter, percent buried volume ($\%V_{bur}$). By obtaining a single crystal of a given organometallic complex, the steric encumbrance of the organic ligands on the metal center may be quantified. Using literature values for $\%V_{bur}$, this project has three fundamental aims. *Aim 1 is to synthesize a suite of electronically and sterically modified organo–nickel compounds targeting the systematic modification of the percent buried volume of the ligand sphere. Aim 2 seeks to utilize these compounds as catalysts to determine the role of $\%V_{bur}$ on product distribution of allylbenzene isomerization. Finally, Aim 3 will investigate the kinetics of isomerization as a function of the $\%V_{bur}$ to determine initial rates of allylbenzene isomerization with organo–nickel complexes.*

Motivating Nickel Isomerization

Alkene isomerization reactions are a fundamental tool for synthetic chemists to create complex organic compounds from simple starting materials.[1,2] The carbon–carbon double bond is a common center for functionalization by a variety of reagents; however, alkene geometry can impact overall reactivity. Alkenes are defined by the rigidity of the double bond, coming in either *E* or *Z* forms. Utilizing isomerization as a method to modify either the positional or geometric identity of the alkene is thus a prevalent and important area of synthetic chemistry. In positional isomerization, the position of the starting alkene is moved along the alkyl chain (Fig. 1).[4] In geometric isomerization, the E/Z geometry is altered (Fig. 1). In this project, we are focused on selective, positional isomerization.[4] Current catalytic systems focus on selectivity about

the double bond, reducing unsafe or otherwise unfavorable reaction conditions, and minimizing side reactivity.[1]

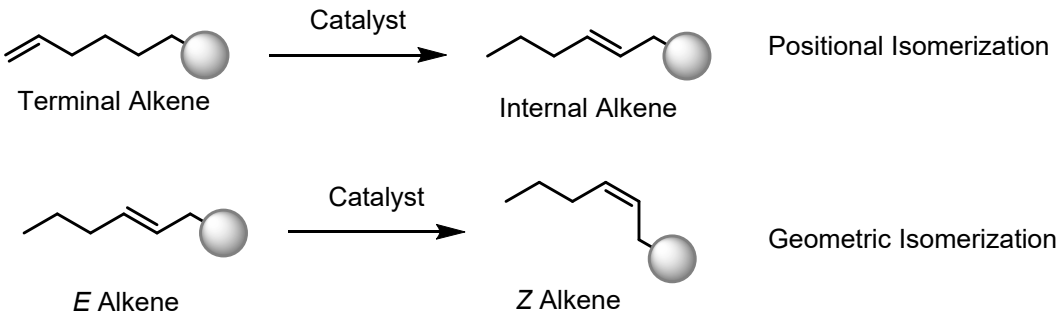

Fig. 1. Positional vs. geometric isomerization.

Allylbenzene isomerization is a vital tool in the chemical industrial setting. The most basic member of the phenylpropanoids, allylbenzene is a molecular scaffold and starting material for a variety of more complex molecules used as perfumes, pesticides, and for their medicinal antifungal properties.[1] Industrially, these products are preferably obtained using base–mediated conditions rather than transition metal catalysis.[1] Base–mediated isomerization, however, is inherently problematic due to harsh reaction conditions. While the base itself can be corrosive or otherwise dangerous, isomerization with base often requires stoichiometric amounts of base or higher loading (e.g., 2–10 equivalents of KO^{t}Bu per alkene) compared to transition metal catalysts.[1,5] Stoichiometric reagents are required in the same equivalence as the starting material and thus consume more chemical starting materials and create larger amounts of byproducts. Additionally, many basic systems rely on refluxing solvent or elevated temperature (≥300 °C).[5] Under such harsh conditions, the energy cost of the reaction increases and the thus the overall efficacy decreases. Ideally, chemical reactions could run with little to no energy input and still maintain selectivity and reasonable reaction times. Basic systems commonly report lower E/Z selectivity as well (10:1 E:Z).[1] By losing 10% of

the product to Z–isomer side reactivity, a significant portion of starting material becomes waste, especially on large scales. The key benefit of base mediated isomerization is the ability to run solventless. The largest competitor to base mediated isomerization are transition metal catalyzed systems.

Transition metal catalysts are well–studied in the literature as potential targets to promote alkene isomerization. Second– and third– row transition metals are commonly employed in isomerization reactions and catalytic reactions in general with the use of platinum,[6] palladium,[7] and iridium,[8] being some of the most well studied.[1,4] While often effective, these metals are expensive and rely on nonrenewable, precious metals. Additionally, some systems have seen reduced E/Z selectivity or promote unfavorable side reactivity.[1] As such, finding cost effective, environmentally friendly alternatives based on these systems is critical and they serve as models for continued work in the field. First–row transition metals are the favored choice because they are cheap and earth–abundant. Cobalt,[9,10] nickel,[2,12,13] and iron[14] have all been reported as effective metal catalysts with mixed results in terms of selectivity, yield, and substrate scope.

Two relevant nickel systems directly motivate this work. In the 1970s Tolman discovered that tetrakis triethylphospite nickel hydride, or, $HNi[P(OEt)_3]_4^+$, generated *in situ* from $Ni[P(OEt)_3]_4$ and H_2SO_4, isomerizes butene derivatives.[13] Tolman's isomerization rearranged the alkene positionally yielding 2–butene from 1–butene (Fig. 2).

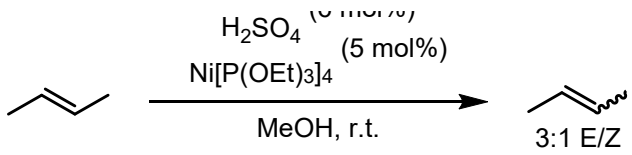

Fig. 2. Tolman's nickel tetrakis catalytic system

The reaction is an example of *in situ* active catalyst generation successful under mild conditions (25 °C).[13] *In situ* generation of the active catalyst simply refers to generating the key reactive species in solution. The mechanism was determined using deuterium labeling and identified a nickel hydride (Ni–H) species as the active catalyst.[13] Tolman employed H_2SO_4 as the hydride source and found the reaction to be dependent on the concentration of acid in solution.[13] While effective, addition of acids potentially limit substrate scope.[1,13] Notable about the $HNi[P(OEt)_3]_4$ catalyst is the phosphite ligand sphere. Additionally, this example of nickel catalyzed isomerization yielded low E/Z selectivity (3:1).[13] More recent advances have been made in the field; in particular, attempting to increase yield and selectivity. In 2018, the Maschmeyer group used the same catalyst as Tolman to investigate reaction kinetics.[14] They faced similar issues in terms of selectivity, forming a mixture of the two products.

More recently, Shoenebeck reported the use of a nickel catalyst for alkene isomerization.[2] Shoenebeck utilized a nickel dimer to selectively isomerize to the E alkene with high to excellent selectivity and yield (>99%, 99:1 E:Z) over a wide array of alkene substrates (Fig. 3).[2]

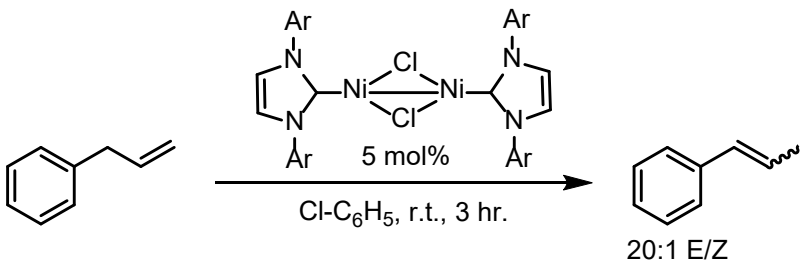

Fig. 3. Shoenebeck's nickel dimer catalytic system

The mechanism was determined using a radical clock experiment and thus confirmed to follow a hydrogen atom transfer pathway (Fig. 4).[2] Because the system did not rely on a Ni–H species, no additives were required and the reaction was completed under mild conditions in reasonable time (room temp, 3 hr.).[2] Additionally, the ligand sphere for Shoenebeck's system provides motivation for our catalyst design. It was reported that an N–heterocyclic carbene (NHC) was coordinated to the nickel dimer.[2] The NHC ligand has been utilized across catalysis literature as a modular ligand for catalysis with several tunable sites. While the Shoenebeck system achieved success with the nickel dimer, much work is left to be done in the field of nickel catalysis. Applying their work to monomeric systems can facilitate studies of the ligand sphere and the role of sterics and electronics on nickel catalyzed systems. Additionally, kinetics and rate law determination will provide important information regarding nickel systems. The single example of a successful, tolerant, nickel catalyst creates the groundwork for broadening the array of nickel species and eliminating those that rely on stoichiometric additives or harsh conditions.

With Tolman's and Shoenebeck's work in mind, we have proposed a nickel monomer species including an NHC ligand sphere to promote allylbenzene isomerization. Previous work by graduate students in the lab has provided precedent for

a Ni–H insertion elimination mechanism (Fig. 4) which required a hydride source. Rather than use a strong acid as Tolman had done, it was proposed that substituted silanes would be more favorable. Silanes are a ubiquitous material in synthetic chemistry used in functionalization reactions for coatings, pharmaceuticals, and other synthetic applications. Several improvements are made when using a silane over a strong acid. Primarily, harsh conditions are avoided which can improve substrate compatibility beyond allylbenzene. Additionally, silanes are a commercially available, cheap starting material. Relying on the silane does not increase reaction cost beyond appreciable amounts. Chemically, silanes are modular, tunable hydride sources. By changing the –R groups, reactivity can be altered thus leading to a more diverse system with regards to tuning the rate and selectivity. Nickel has been seen as an active hydrosilylation catalyst[3,4,11] with groups trying to mitigate the isomerization reactivity in their systems. In particular, Chirik et. al. recently showed via deuterium labeling that deuterium incorporation occurred across an entire alkyl chain during the hydrosilylation of 1–octene.[16] The reason for such incorporation was isomerization during the hydrosilylation reaction which provides definitive proof of concept for the use of silanes in nickel–mediated isomerization. We use this precedent as motivation for the implementation of hydrosilanes as a mild alternative to acid hydride sources.

Current Mechanistic Understandings of Isomerization

There are three, common transition metal–catalyzed isomerization pathways.[12] The reaction can follow a hydrogen atom transfer, metal–hydride insertion–elimination, or η^3–allyl pathway (Fig.4).[2,12]

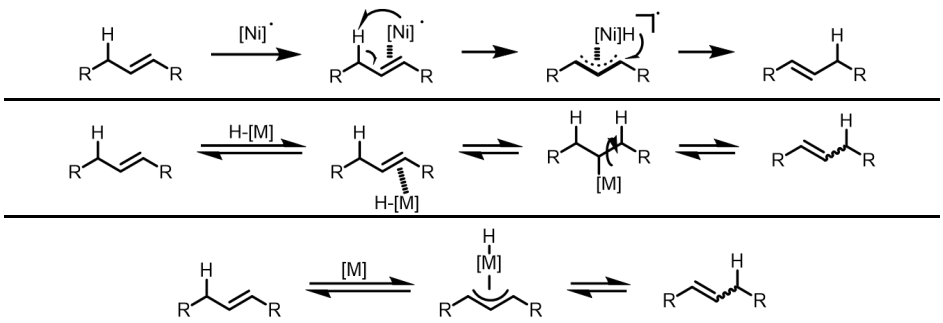

Fig. 4. Common isomerization mechanisms. Hydrogen atom transfer (**top**), metal hydride (**middle**), η^3–allylhydride (**bottom**).

In the second two cases, the alkene coordinates to a metal center, however, the means of coordination varies. As such, the two methods form unique and important intermediates that effect the method of rearrangement. In the metal–hydride mechanism, a hydrogen from the metal site is donated to the alkene, however in the η^3–allylhydride pathway, the metal inserts itself between a hydrogen originating on the reactant, thus forcing rearrangement.[12] Importantly, the metal–hydride mechanism relies on an external hydride source whereas the η^3–allylhydride simply rearranges a hydride already on the reagent. The external hydride source is a critically important factor in metal catalysts that undergo the hydride insertion–elimination mechanism and is a key feature in those systems. In the radical mechanism, a metal radical abstracts a hydrogen atom, forming an allyl radical species that then rearranges and reforms the alkene in a new position.[2] Alternatively, given a pre–exsisting metal–hydride, hydrogen donation could be the first step in a radical mechanism.[9] After donating to the substrate in a radical mechanism, a second hydrogen would then be abstracted to form the product.[9] To determine which mechanism is dominant, one can run a series of experiments including deuterium–labelling studies, kinetic investigations, or design reactive substrates that target specific

groups such as radicals. The deuterium labeling method is the most straightforward because different hydrogens are used in the two pathways.[12]

With first–row transition metals such as cobalt and nickel, metal–hydride insertion–elimination is the most common of the three pathways.[12] Mechanistically, the metal–hydride insertion pathway is well known and has multiple important steps.[1,12] By examining each step, we can better hypothesize how altering the ligand sphere of the metal catalyst might change the product distribution. The complete, proposed metal–hydride isomerization catalytic pathway is detailed below in Fig. 5.

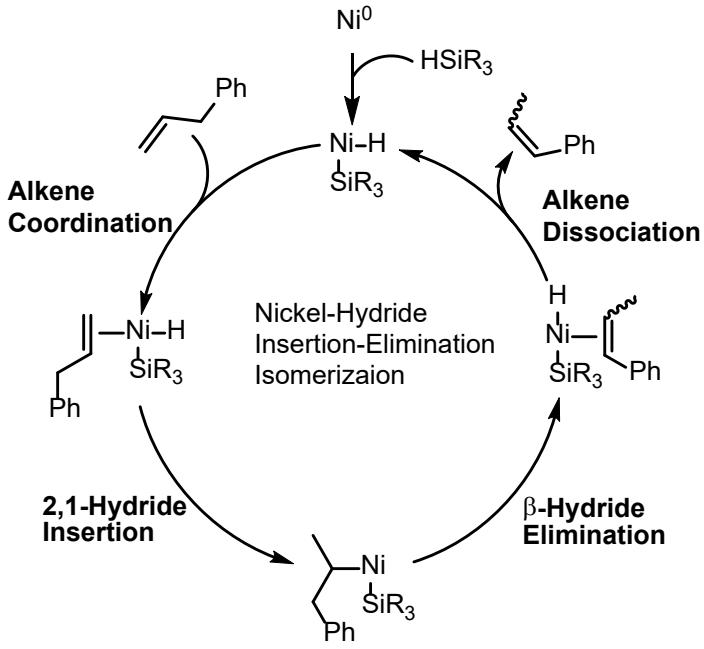

Fig. 5. Nickel–Hydride Insertion–Elimination Isomerization Mechanism

In the scheme, a silane is used as the hydride source. The reaction begins by forming the proposed active catalyst, a nickel hydride, via oxidative addition of a silane. Note that the oxidation state of the active catalytic species is a Ni(II) complex contrasted by the precatalyst which is a Ni(0) complex. Coordination of the proposed alkene substrate follows production of the active catalyst. From here, a [2,1]–insertion step creates a new

Ni–C bond and protonates the alkene. Reductive elimination between the Ni–C bond repositions the alkene on the carbon chain and creates the product, still coordinated to the metal center. Finally, the isomerized alkene dissociates from the metal and the active catalyst is regenerated, thus completing the cycle. The organic moieties are not shown; however, it is hypothesized that they impact the product distribution. Formation of the alkene during reductive elimination is the key step where geometry about the final alkene product is defined.

This Work

Metal catalysts are distinguished by the organic moieties surrounding them. Dubbed the ligand sphere, the organic ligands define the reactivity of the catalyst and will be the key feature we seek to modify. Ligands can contribute either steric or electronic effects to the metal complex. Sterics consider the physical, spatial area occupied by the ligand. A physically larger substituent is considered to have larger steric bulk. Electronics are much more complex and rely in part on electronegativity trends of the elements. Atoms such as fluorine and chlorine are strongly electron–withdrawing while alkyl (C–C) groups are generally electron–donating. Ligand electronic and steric factors define the reactivity of the catalyst, and we want to quantitively define their effect. As such, we have postulated four nickel compounds (**1a-4a**) that we seek to synthesize that will help determine the role of steric factors in catalytic isomerization. Our targeted complexes are pictured in Fig. 6.

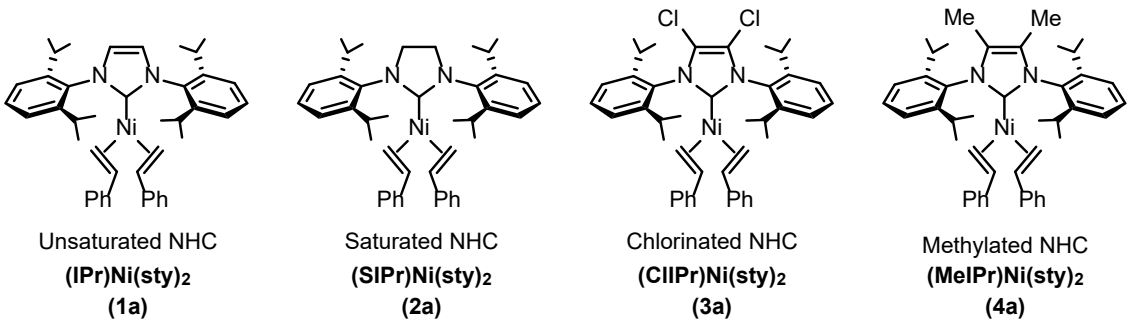

Fig. 6. Proposed synthetic nickel complexes for isomerization

By modifying the backbone of the N–heterocyclic carbene (NHC) ligand on the "top" of the nickel complex, we can quantify the effects of steric changes. The sterically smallest complex and thus the "parent" will be the unsaturated NHC, **1a**. From there, we increased steric bulk by saturating the backbone with hydrogen, **2a**. Adding chlorine groups, **3a** further increased sterics and adding the CH_3 groups, **4a** created the bulkiest substituent.[17] These modifications will be compared to the unsubstituted, unsaturated NHC, **1a**. The proposed changes in complex size can be quantified using the percent buried volume of the molecule.[17] Percent buried volume ($\%V_{bur}$) is a quantitative measurement of the spatial crowding that a ligand creates when coordinated to a metal site.[17] The measurement is made using a single crystal analysis to achieve an exact structure for the molecule in question.[17] The map made from the crystal structure can provide exact measurements regarding bond distances, bond angles, and most importantly, $\%V_{bur.}$[17] In 2018, the Louie group synthesized the targeted complexes as well as a variety of other Ni(NHC) complexes and calculated their $\%V_{bur}$.

In their paper, the Louie group found that the expected size trend held with respect to $\%V_{bur}$. That is, the methyl substituents created the largest $\%V_{bur}$ while the unsaturated complex (**1a**) had the smallest ligand sphere.[17] The Louie group also concluded that the N–C_{ar} bond angle and the metal–ligand cone angle both become

more strained as crowding increased.[17] Using the values for $\%V_{bur}$ calculated by Louie et. al., we were able to directly equate steric influence to product distribution in terms of both overall yield and E/Z selectivity. *It is hypothesized that increasing the bulk will decrease overall yield while simultaneously increasing selectivity for the Z product. We think that increasing steric bulk will decrease the size of the open coordination site on the nickel complex and thus hinder catalytic activity. Additionally, the sterics may force the geometry about the double bond to relieve crowding.*

Proposed Synthetic Steps

While hypotheses about reactivity are inherently useful, first the ligands needed to be synthesized. Synthesizing the ligands of interested was a large portion of the project. Luckily, synthetic pathways have been established in literature to provide a starting point. Unfortunately, no single paper provided a list of steps to achieve all our desired compounds. As such, one goal of this work was to provide a compilation of synthetic steps to reach the target complexes. The general schemes followed are outlined in Fig. 7.

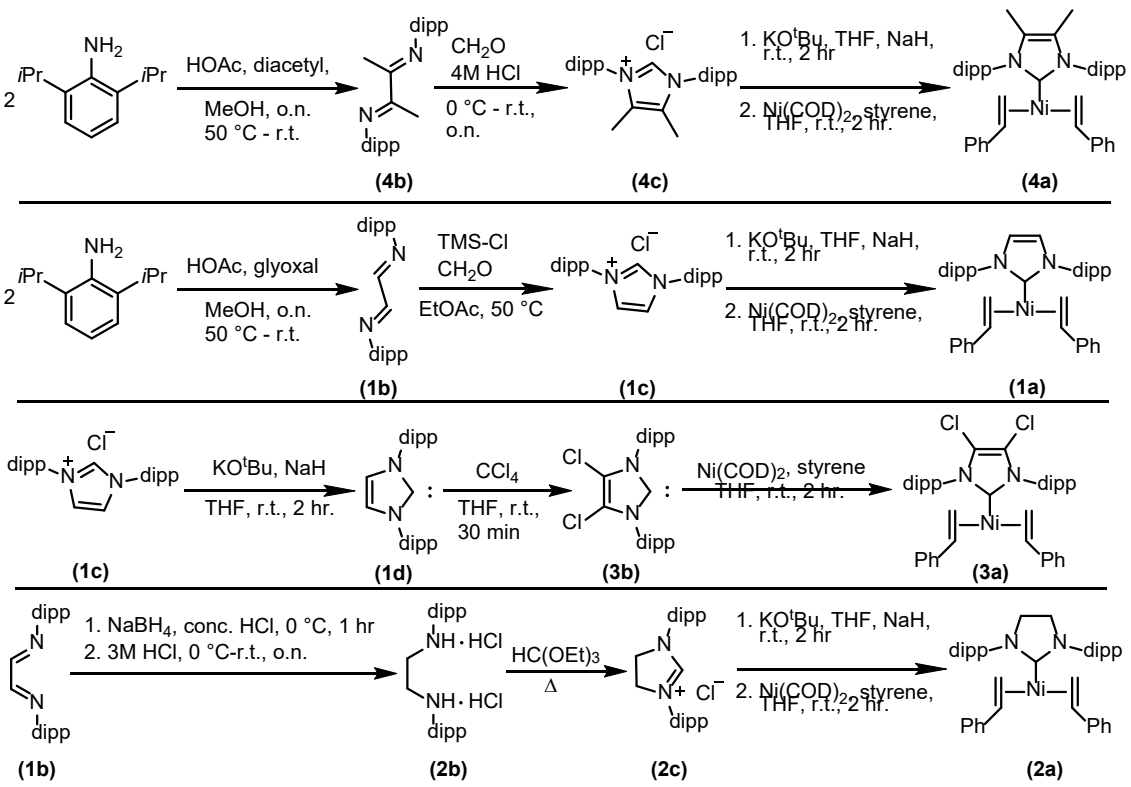

Fig. 7. Known synthetic pathways for target nickel complexes

To make the unsaturated NHC **(1a)**, Bantriel provided a facile synthesis.[19] Starting from glyoxal and substituted aniline, both cheap and available starting materials, Bantriel first makes the substituted diazadiene **(1b)** in a condensation reaction.[19] From there, formaldehyde is added to close the ring and form the imidazolium salt **(1c)**.[19] To facilitate later deprotonation, an ion exchange from the halide to a tetrafluoroborate is undergone, however this step is not shown in the scheme above (**1e)**. Finally, a deprotonation step results in the desired NHC ligand **(1d**. To coordinate to the nickel center, a ligand exchange reaction can be achieved using a strong base such as NaH or KO^{t}Bu or both.[19] Addition of NaH promotes the formation of H_2 gas thus limited reversibility of the reaction. Bantriel shows this process to be available for both alkyl and aryl substituted substituents.[19] While the other three ligands have all been shown by Arduengo, their synthesis required dangerous reagents.[20,21] As

reported by Arduengo, the initial steps to the NHC for both the methyl– and chloro–substituted products **(4a, 3a)** are identical to those shown by Bantriel.[20,21] Further reactivity differs however to get the individual products with varied backbones.[20,21] Despite the seemingly simple operation of functionalizing the NHC backbone, using monochloromethane is dangerous and unfavorable. Instead, starting from diacetyl, rather than glyoxal, allows for formation of the methyl NHC **(4a)** by similar reactions as the parent ligand. These reactions, however, have never been reported cohesively in a single paper and the yields are low for important steps. Arduengo recommends the use of diacetyl in identical conditions reported with glyoxal to achieve the diazadiene **(4b)**, however reports no further synthetic steps.[20] From the methylated diazadiene **(4b)**, Beillard reported the use of HCl rather than Bantriel's TMS–Cl to achieve ring closure **(4c)**.[22] While useful, these conditions produced a relatively low reported yield of 23%.[22] Thus, it would be prudent to optimize conditions and adapt purification techniques to increase the yield of the methylated imidazolium chloride **(4c)** and achieve a higher yield. The saturated NHC ligand **(2a)** is different and requires unique steps throughout once the diazadiene **(1b)** is made. To achieve the saturated compound, **(2a)** the Hans group provided simple, high yielding syntheses.[23] Starting from the diazadiene **(1b)**, protonation could be achieved using sodium borohydride and concentrated HCl.[23] The resulting dihydrochloride salt **(2b)** could then be easily closed into a saturated imidazolium chloride **(2c)** using heat, triethyl orthoformate, and HCl.[23] Despite the synthetic ease of achieving the saturated imidazolium chloride, the final ring closure **(2c)**, as reported by Hans, required the use of a high–powered microwave unavailable to our lab and thus potentially unavailable to other labs seeking the same compound.[23] As

such, it was hypothesized that the microwave could be circumvented by longer reaction times and modified steps based on similar reactions with different substrates.[24] Overall, while the complexes have been reported prior to this work, it was recognized that synthetic routes to this fundamental scope of sterically modulated NHC ligands were not easily accessible. *As such, this work sought to collect and improve upon NHC synthesis via traditional organic chemistry techniques.*

Methods

Herein, it is my objective to outline the synthetic techniques that I used to synthesize the complexes of interest. While most of these synthetic pathways have been reported prior, I found that the literature reactions were sometimes unproductive, low–yielding, or otherwise needed to be modified to achieve the highest level of success and purity. Additionally, it is important to define and outline the common techniques used in synthetic laboratories to familiarize outside readers with their uses and importance.

Synthesis

Traditional organic synthesis techniques were used to create the ligands of interest. These techniques included extraction, separation, and drying of compounds using a rotary evaporator or Schlenk line vacuum/liquid nitrogen trap. The rotary evaporator is a tool that allowed for the separation of liquids and dissolved solids/oils by boiling the liquid off and collecting the residue left behind. The Schlenk line is a tubing system used for air or water sensitive reactions. Heated glassware was attached to the Schlenk line and placed under vacuum to remove the O_2 then refilled with inert N_2. As previously mentioned, ligand synthesis required multistep reaction schemes that could take several days to complete. After each step, the products were dried, purified, and characterized to ensure confirmation of the molecular identity.

Compound purification relied primarily on trituration or solvent washes, recrystallization, or column chromatography. Ligand impurities proved incredibly detrimental because they altered reactivity further down the synthetic pathway. For example, imidazolium chloride with impurities proved entirely unreactive towards deprotonation until the impurities were removed. Most impurities were separated via

differences in solvent solubility however, occasionally, more involved purification was required.

Column Chromatography

Column chromatography was one avenue used to rigorously purify the alkene substrates of interest; however, it was never used on ligands. Column chromatography works by making a slurry of silica gel in a mixture of polar and non–polar solvents. By pushing compounds through the solution, we were able to separate desired products and their impurities. Due to electronic effects within the molecules, products and impurities run through the slurry at different rates making them easy to separate. The impure product was dissolved in a predetermined mixture of a polar and a nonpolar solvent (e.g., diethyl ether and hexanes, respectively) then run through the silica gel column. As the impurities are separated, aliquots were collected and analyzed for what they contain. Once all the impurities or products had run through, the pure aliquots were collected and concentrated using a rotary evaporator.

Recrystallization

Solvent washes and recrystallizations were a significant method of purification for the ligands themselves. Once synthesized, many of the products were either semi–soluble or entirely soluble in the reaction solution. Solubility is dramatically affected by temperature though and, on such occasions where the product was partially soluble in its reaction solvent, cooling the mixture to below 0 °C worked to precipitate the desired solids. When collecting precipitate in this manner, using solubility differences, a crystalline product is often formed, and the process is thus dubbed recrystallization.

Once product was observed, either via recrystallization or immediately out of the reaction flask, the precipitate was collected over a glass frit using vacuum filtration. Solvent washes were used to remove any remaining impurities and the resulting powder was dried on a high–powered vacuum between one hour and up to overnight before being used in the next synthetic step.

^{1}H–NMR Spectroscopy

After purification had been completed, the products were characterized using primarily ^{1}H nuclear magnetic resonance (NMR) spectroscopy. The structural characterization of products is crucial to confirm product formation before advancing to the next synthetic step. NMR spectra are unique to each molecule with positionality, line shape and coupling constant between peaks representing distinct, identifiable atom environments. NMR works by magnetically exciting the spin state of a given, odd–numbered atomic nucleus from the $m = -\frac{1}{2}$ to the $m = \frac{1}{2}$ state and tracking the return to a relaxed state. Since the response is dependent upon chemical environment, different atom environments produce unique signal peaks that can be assigned to respective positions within a molecular structure. By going through the peak assignment process, each molecule was distinctly characterized, and any impurities can be observed.

Once the target organic ligands were synthesized, they were treated with a nickel complex to form the desired nickel complexes, which were air– and water–sensitive, thus requiring the use of either an inert gas glovebox or a Schlenk line. In the glovebox, large scale reactions can be completed without the fear of air or water contamination. For this project, a nitrogen gas glovebox was used. Reagents and solvents were rigorously purified prior to use in these sensitive reactions. All liquid

reagents and solvents were prepared for the glovebox through distillation and freeze–pump–thaw methods or dispensed from a solvent purification system. As with the organic precursors, we thoroughly characterized our inorganic products using the techniques stated above. The complete, detailed, synthetic protocols for each compound with NMR spectra attached can be seen in the Supplementary Information.

Catalyst Screenings

The final nickel compounds were studied in the model isomerization reaction of allylbenzene to β–methyl styrene. Allylbenzene is a parent molecule to a variety of other more functionalized and industrially useful compounds such as safrole, eugenol, or chavicol (Fig. 8).[2]

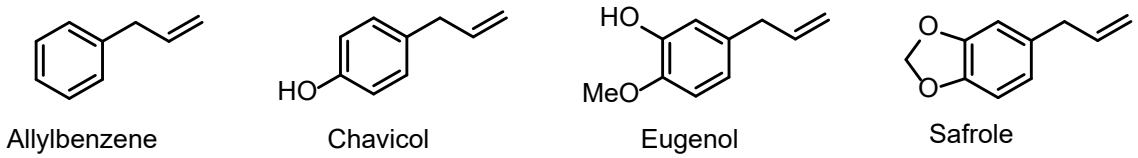

Fig. 8. Allylbenzene as a parent compound to more diverse substrates

Previous work by graduate students in the lab found optimized reaction conditions for allylbenzene isomerization. These conditions saw all nickel screenings run in either toluene or hexanes at 70 °C or 80 °C. Scintillation vials were charged with catalyst in a nitrogen glovebox completely free of air and moisture. To these vials, durene was added as an internal standard along with the silane to act as a hydride source. We loaded all experiments on the 5 mol% catalyst scale with a 1:1 ratio of Ni to silane due to previous work in the lab proving this to be the ideal loading condition. Once made, the vials were capped with permeable septum caps and brought out of the box. The reactions were

heated for 30 minutes to facilitate formation of the proposed Ni–H active catalyst before allylbenzene was added via a microsyringe.

Gas Chromatography

Once complete, product distribution was analyzed using gas chromatography. Gas chromatography (GC) is a method of compound characterization that utilizes the molecular weight of the desired molecule. In GC, a liquid sample of the reaction mixture is passed through a column containing a carrier gas that separates the chemicals based on chemical adsorption similar to the column chromatography purification method. Based on the relative molecular weight, different compounds elute at different time intervals and produce signals across a spectrum of seconds or minutes. Thus, any compounds present in solution can be characterized by their relative intensity and time interval. After elution, a flame ionizing detector is used to ionize the molecules as they exit the column. The spike in voltage due to ionization creates the signal that is measured. Using GC, we were able to accurately understand all isomerization products as well as their relative yields thus producing a quantitative measurement regards product distribution between E and Z isomers as well as any side products or starting material left over.

Results

With the target complexes fully synthesized and characterized, isomerization reactivity could be probed. A common alkene substrate for isomerization reactivity is allylbenzene, shown as **(1)** in Table 1. Despite its chemical relevance as a parent molecule to other more complex alkenes, practically, allylbenzene is an ideal substrate. Allylbenzene is easily characterizable and promotes little side reactivity, making it an useful for general tests. Additionally, the alkene only has one possible positional isomerization product as either an E or Z alkene. Thus, it provides a model substrate for determining the favored geometry of a given catalyst. Examining the catalytic cycle, the proposed mechanism undergoes [2,1]–insertion with a hydride. We chose triphenylsilane as the hydride source with the hopes of promoting further reactivity that will be discussed later.

Overall Yield and Product Distribution

Reactions were set up with 5 mol % catalyst loading in toluene, heated at 80 °C for 16 hours to probe selectivity and yield. The reaction conditions were optimized prior to this study by a graduate student in the group. Toluene was used to facilitate solubility of all reactants and they were done in duplicate to ensure repeatability. Reaction conditions and product distributions are tabulated below in Table 1.

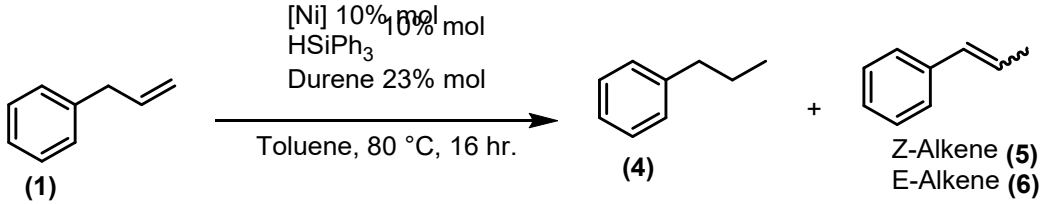

Entry	NHC	*Product Distribution (%)* 1 : 4 : 5 : 6	Alkene yield (%)	*E*/*Z* ratio
1	^{Me}IPr	0 : 2 : 4 : 84	88	21:1
2	^{Me}IPr	0 : 2 : 4 : 90	94	20:1
		Average:	91±3	21±1:1
3	^{Cl}IPr	0 : 1 : 4 : 80	84	21:1
4	^{Cl}IPr	0 : 1 : 4 : 81	85	21:1
		Average:	85±1	21±0:1
5	SIPr	3 : 1 : 10 : 75	84	7:1
6	SIPr	5 : 1 : 9 : 66	75	7:1
		Average:	80±5	7±1:1
7	IPr	0 : 1 : 4 : 95	95	21:1
8	IPr	0 : 1 : 4 : 87	87	21:1
		Average:	91±4	21±1:1

Table 1. Isomerization of Allylbenzene

All complexes showed a preference for the E isomer **(6)** over the Z isomer **(5)** as determined by GC. The E isomer elutes later than the Z isomer thus it is easily distinguishable. All complexes also displayed side reactivity creating product **(4)**, the hydrogenated alkane. This side reactivity is undesirable and limited in all reactions, however the SIPr **(2a)** complex showed a higher propensity for the hydrogenated side product. As such, overall, the SIPr **(2a)** catalyst performed the worst in terms of yield, selectivity, and side reactivity.

First, examining overall yield provides a meager trend. The MeIPr (**4a)** complex showed the greatest yield, and as sterics decreased, so did yield. Contrary to this trend, the parent IPr **(1a)** complex showed equivalent yield to the MeIPr **(4a)** complex despite the largest difference in $\%V_{bur}$. This observation is intriguing because it contradicts the trend exhibited by the other complexes. Examining the catalytic cycle, (Fig. 5), it was

hypothesized that sterically bulky ligands would limit the size of the coordination site thus reducing availability for alkene coordination and further isomerization. This hypothesis, however, has been proven incorrect by the results. Regardless of steric size, overall yield remained high with all complexes with decreased yield from complexes with smaller ligand spheres. Additionally, selectivity was largely unchanged regardless of size. There is virtually no trend in selectivity, other than it can be concluded that the SIPr **(2a)** complex showed significantly deteriorated selectivity. These catalysts performed admirably with regards to selectivity and yield. The observed 21:1 average preference for the E alkene over the Z alkene is comparable to literature for other nickel complexes.[1]

Quantitative analysis is important for elucidating any sort of trend in isomerization activity. Using the values from Louie, we can directly compare $\%V_{bur}$ with isomerization yield and selectivity.[17] Table 2 compares these numbers while Fig. 9 displays them graphically.

Complex	Ni–C_1 Bond Length [Å]	$\%V_{bur}$ (%)	Avg. % Yield (%)
IPr (1a)	1.899	36.9	91
SIPr (2a)	1.897	38.1	80
^{Cl}IPr (3a)	1.910	39.1	85
^{Me}IPr (4a)	1.924	39.6	91

Bond length and $\%V_{bur}$ obtained from Louie et. al.[17]

Table 2. $\%V_{bur}$ and Bond Length compared to Isomerization Yield

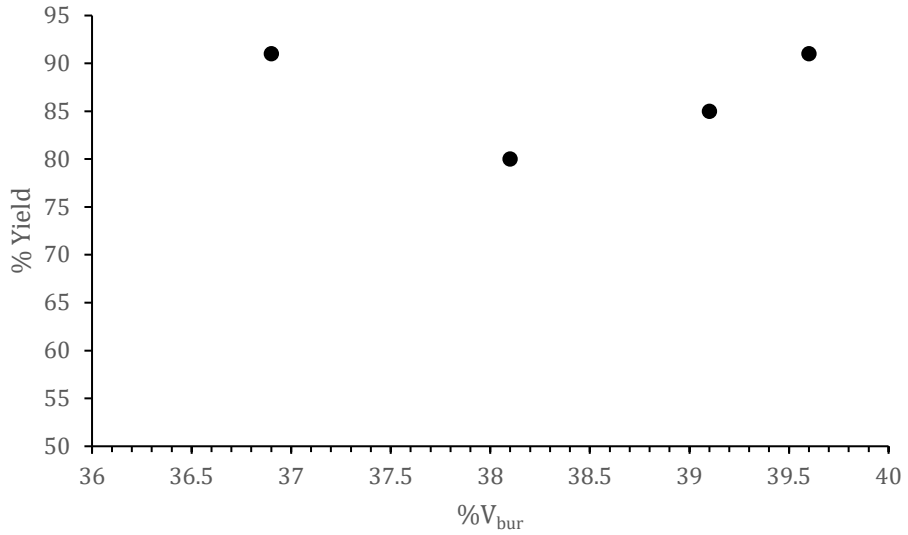

Fig. 9. Graph portraying overall, average % alkene yield against $\%V_{bur}$.

From Fig. 9, excluding the parent complex, there is a strong trend for increased yield as ligand size increases. Despite this, it cannot be concluded that the isomerization yield has any dependence on crowding about the nickel center. The parent complex is far from an outlier and thus dissolves any apparent trend in the data. Additionally, the lack of observable change in alkene selectivity provides evidence that sterics about the ligand sphere have little influence on the formation of isomerized product. These results provide useful information about the role of the ligand sphere in determining product selectivity. Further experiments have been run with data pending regarding the kinetics of the reaction and the effect of the ligand sphere on determining the initial rate of reaction. While formal data is unavailable, it seems as though complexes with more highly substituted ligand spheres achieve full isomerization sooner than those with smaller ligand spheres.

Electronic modulations should also be considered. The effect of electron withdrawing or electron donating groups is equally important to catalyst efficiency.

Methyl groups are electron donors, hydrogen atoms are neutral moieties, and chloride groups are electron withdrawing. Considering these classifications, our complexes span a range of electronic effects with the saturated NHC falling outside this range. The electron donating, and neutral substituted ligands (^{Me}IPr, IPr) performed overall better than the only electron withdrawing substituted ligand (91%>85%). As such, while this is far from rigorous, it shows precedent for the comparison of electron withdrawing groups on the NHC backbone. This simple observation with an extremely tight range of catalysts gives preliminary evidence for electron donating ligands as more beneficial to catalyst efficiency.

Initial Rates of Reaction and Kinetics

Despite the lack of distinct changes in product distribution over 16 hours, rate of reaction is also hypothesized to be altered by the ligand sphere. Larger $\%V_{bur}$ limits the size of the coordination site which led to the hypothesis that the rate of isomerization with more sterically crowded complexes would ultimately be slower. Using the same conditions as the product distribution reaction, a kinetic time study was done on the nickel complexes. The SIPr **(2a)** complex was left out due to the conclusion that unknown impurities were hindering reactivity. The results of the first time study, done at 80 °C are plotted on a graph in Fig. 10.

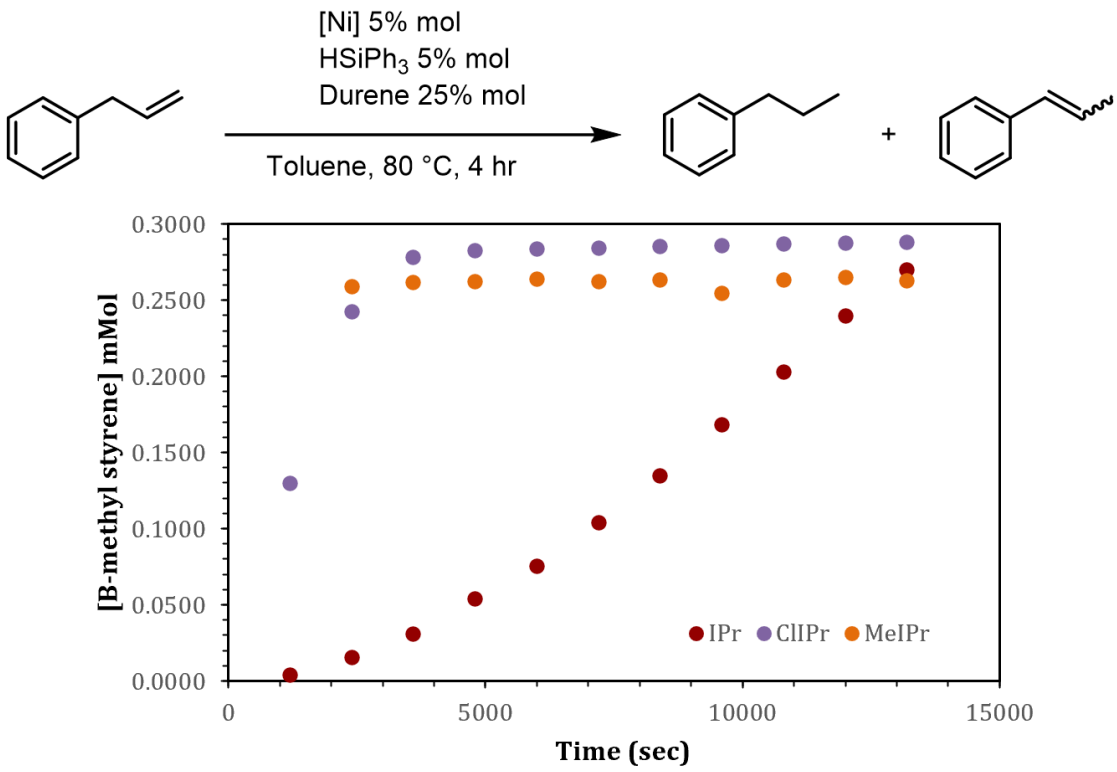

Fig. 10. Concentration of β-methyl styrene over time for the complexes MeIPr, ClIPr, IPr at 80 °C

Contrary to the hypotheses, it was seen that the parent IPr **(1a)** complex performed isomerization with the slowest rate, taking the entire 4 hours to reach completion. The MeIPr **(4a)** and the ClIPr **(3a)** completed reactivity much faster with the methylated complex **(4a)** reaching full conversion after merely 40 minutes and the chlorinated complex **(3a)** reaching full conversion after 60 minutes. Similar to the product distribution hypothesis, complete reversal of expectations was seen for the rates of reaction. The most sterically bulky ligand performed isomerization the fastest while the least sterically bulky ligand performed much slower. Initial rates were impossible to determine from these data points, however, due to the rapidity of reaction at 80 °C. As such, the temperature was decreased, and kinetics were run again at 70 °C in toluene

(Fig. 11). Rather than take 20 minute time points as was done with the trials at 80 °C, time points were taken every 5 minutes. Data for the IPr **(1a)** complex was only analyzed every 30 minutes due to the significant decrease in overall yield at 70 °C. It is so far unconfirmed if the observed decrease corresponds to catalyst reactivity or rather reaction quenching due to the introduction of oxygen into the vials.

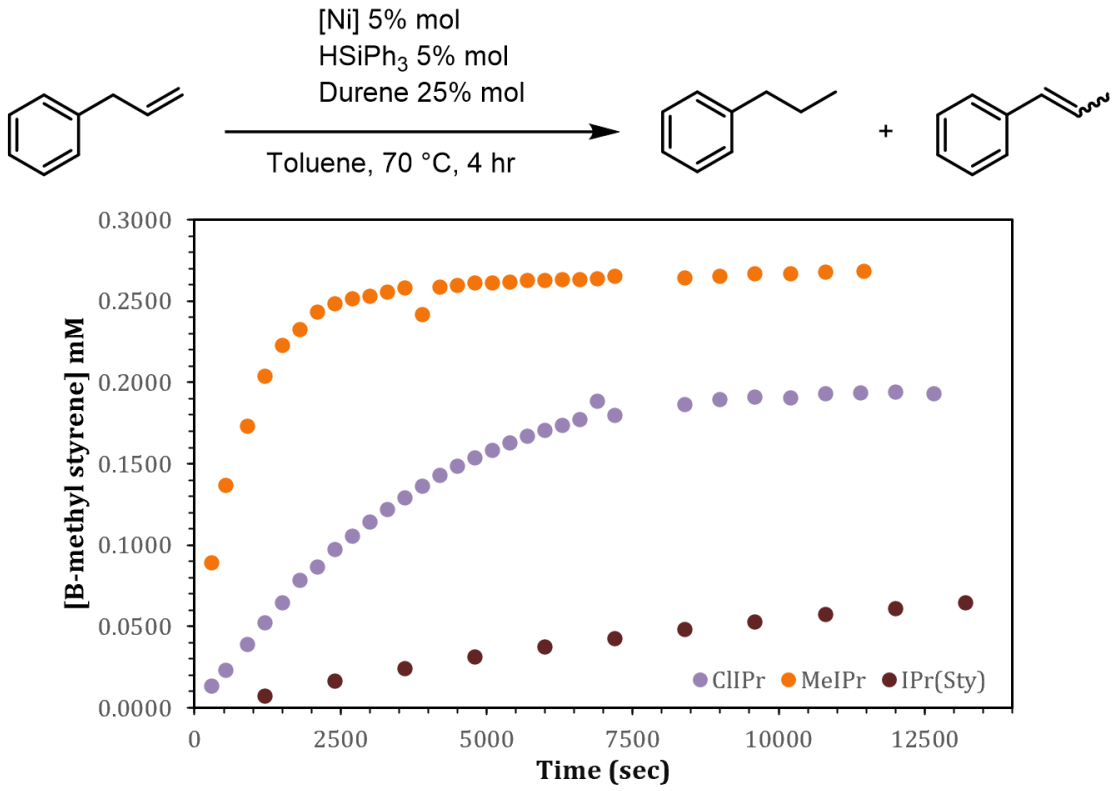

Fig. 11. Concentration of β-methyl styrene over time for the complexes MeIPr, ClIPr, IPr at 70 °C

With the reactions run at 70 °C, overall product yield was diminished in all catalysts. Yields plateaued near 80% for the MeIPr **(4a)** complex and 55% for the ClIPr **(3a)** complex. The parent, unsubstituted nickel–IPr **(1a)** complex was unable to reach a plateau within the 4–hour window. Regardless, the kinetic profiles achieved still facilitate determination of the initial rate of reaction. By plotting a linear fit to the

initial, linear data within the kinetics trials, we retrieved quantified measures of the rate of reaction. Data points were selected prior to reaction plateaus such that the R^2 values of the regression fitting were minimized within reason. The initial rates of isomerization at 70 °C are tabulated in Table 3.

Complex	$\%V_{bur}$ (%)	Initial Rate of Reaction (M/s)
IPr (1a)	36.9	5.05×10^{-6}
^{Cl}IPr (3a)	39.1	4.05×10^{-5}
^{Me}IPr (4a)	39.6	1.20×10^{-4}

Bond length and $\%V_{bur}$ obtained from Louie et. al.[17]

Table 3. $\%V_{bur}$ and Bond Length compared to Initial Rates of Isomerization

Based on the calculations reported in Table 3, it was seen that the initial rate of reaction for the MeIPr **(4a)** complex was significantly larger than that for the ClIPr **(3a)** and IPr **(1a)** complexes. Quantitatively, the MeIPr **(4a)** complex isomerized allylbenzene 2.96 times faster than the ClIPr **(3a)** complex and 23.76 times faster than the IPr **(1a)** complex. As such, a larger ligand seems to promote isomerization faster and achieve a greater overall yield. With regards to selectivity, the changes in temperature had no influence and high E/Z selectivity was seen in all kinetic studies (>26:1 E/Z). Formation of the hydrogenated byproduct was seen in 2% yield for all substrates. This is considered an insignificant amount considering the rapidity and success of the complexes towards selective E isomerization.

Future Directions/Conclusion

This work had three fundamental aims. The first was to establish synthetic protocols for a range of sterically modulated NHC–nickel–styrene complexes. This first aim was met entirely. Synthetic routes from literature were dramatically improved upon with regards to both yield and ease of set up. In particular, yield of the methylated imidazolium chloride ([1,3–Bis(2,6–diisopropylphenyl)–4,5–dimethyl]imidazolium chloride) **(4c)** was improved upon dramatically by reconsidering purification methods. Literature reported 23% while we regularly achieved >50% yields.[22] Thus, we were able to effectively double the retrievable yield from the reaction. Additionally, the use of complex and expensive equipment was mitigated in the synthesis of the saturated imidazolium chloride **(2c)**.[23] While literature protocols rely on microwave synthesis, we were able to achieve high yields (99%) by using common organic laboratory glassware.[23] These two synthetic achievements, combined with the compilation of the successful, total synthetic routes to fundamental NHC complexes have satisfied the expectations set out by Aim 1 of the project.

Moving forward synthetically, creating a range of new NHC complexes would be an important step for ligand design. Unlocking previously unmade NHC compounds with varied backbone architectures would facilitate a wide range of catalytic studies in both sterics and electronics. With regards to steric modifications, larger moieties could be applied to the backbone such as substituted or unsubstituted phenyl groups, larger halogens, or longer alkyl chains. While this work examined an established range of complexes varied systematically with regards to $\%V_{bur}$, an even wider range of steric modifications would be useful for more deeply understanding the role of the ligand

sphere with regards to many catalytic reactions. Precedent was seen for increased sterics increasing both overall yield as well as initial reaction rate. This could be verified by further increasing ligand sterics. These studies, however, would be impossible without efficient synthetic protocols. Additionally, modulating the backbone of the NHC with more electron withdrawing or donating groups would be useful. Synthetic routes to these ligands will be studied in the future.

Aim 2 of the project sought to quantitatively understand the role of ligand sterics on the nickel catalyzed isomerization of allylbenzene. This was done by examining yield and product distribution as a function of the $\%V_{bur}$ of the catalysts. While the yield seemed to decrease as $\%V_{bur}$ decreased, the saturated IPr complex disobeyed this trend resulting in the conclusion that sterics have little effect on catalyst efficiency. Despite this, there are many reactions that can be tested in the future to achieve a stronger understanding of sterics role on the reaction. Further mechanistic insight could be achieved using deuterium labeling to track proton movement throughout the reaction. Labeling the silane with deuterium would conclusively prove which of the three common isomerization mechanisms is undergone with these catalysts. Finally, with regards to the catalysts, it was seen that the ligands my create an electronic influence as well as a steric one. Thus, modulating the backbone of the NHC with a range of electron withdrawing and electron donating moieties could be a useful examination. As a novel system, understanding every aspect of the catalyst, both with regards to electronics, sterics, product distribution, kinetics, and mechanism are all incredibly important for incorporating the catalyst into industrial processes. This report sought to understand one of the variety of factors that can affect catalytic reactions.

The third project aim was to determine the initial rates of reaction for allylbenzene isomerization with the targeted nickel NHC complexes. This was done successfully for three of the four complexes, but impurities restricted the use of the SIPr **(2a)** complex in kinetics. Regardless, it was observed that increasing the steric backbone greatly increased the initial rate of isomerization and overall yield even at decreased temperature. The MeIPr **(4a)** complex showed incredibly fast propensity for isomerization at 80 °C completing in less than an hour whereas the parent complex took over four hours to reach full product conversion. As such, we have shown that while sterics may not influence E/Z product distribution they greatly influence the rate of reaction. Moving forward with this aim, the first goal would be to test the SIPr **(2a)** complex for its kinetic profile. Additionally, it would be prudent to test a wider range of sterically modified NHC ligands. Precedent has been established for increasing steric bulk and thus increasing reaction rate, but this trend most likely has an optimal range and finding it would be particularly important for establishing the tunability of the catalyst.

The last important direction this project could take examines entirely new reactivity. Utilization of the silane as a hydride source was intentional. A common functionalization reaction in industry is hydrosilylation of an alkene.[3,11] Hydrosilylation is used to create a wide array of products from silicone coatings to diapers.[3,11] Despite its utility, hydrosilylation reactions are currently plagued by side reactivity and low selectivity, similar to isomerization reactions.[3,11] By using a silane as a proton source, we might be able to combine hydrosilylation and isomerization in a tandem catalytic cycle. In doing so, we could optimize both reactions and functionalize previously

unreactive sites on an alkene containing substrate. Thus, the last and more theoretical further direction this project could take would be to study the catalysts made in hydrosilylation reactions, optimizing their effectivity and studying the role of sterics and electronics in this alternative system. By using a single catalyst for a tandem reaction cycle, the potential for efficient, green chemistry is incredibly high.

Supplementary Information

Here, the HNMR data is provided for all complexes and compounds with peaks summarized.

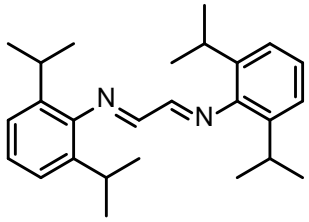

Synthesis of 1PTM – 53: N,N'–diisopropylphenyl–2,3–ethanediimine: (1b) A solution of 2,6–diisopropylaniline (9.5 mL, 50.3 mmol, 2 equiv.) in 50 mL of methanol was heated to 50 °C and charged with acetic acid (0.3 mL, 5.3 mmol, 0 equiv.). To this solution, a second solution of 40% (w/w) glyoxal (2.9 mL, 25.4 mmol, 1 equiv.) in 50 mL of methanol was added slowly over the course of 1 minute. Upon addition of glyoxal, the reaction yellowed and stirred overnight for 20 hr. resulting in the precipitation of a yellow precipitate. The precipitate was collected on a glass frit and dried on high vac to remove water and solvent. Total yield: 6.36 g, (66.5%). ^{1}HNMR (500 MHz, Chloroform–*d*) δ 8.10 (s, 2H), δ 7.18 (m, 6H), δ 2.95 (sept, J = 6.7 Hz, 4H), δ 1.21 (d, J = 6.9 Hz, 24H). TMS at δ 0.0, H_2O at δ 1.51

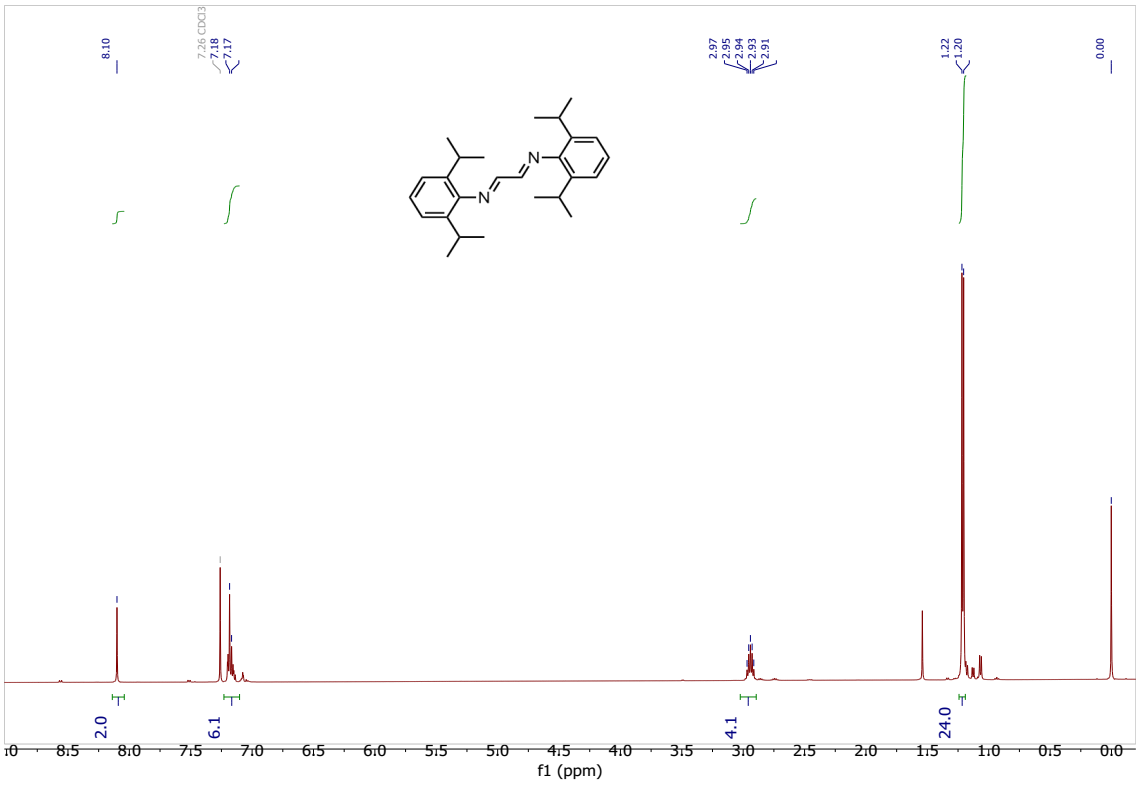

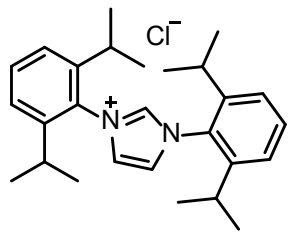

Synthesis of 1PTM – 54: 1,3–Bis(2,6–diisopropylphenyl)–imidazolium chloride:

(1c) A solution of N,N'–diisopropylphenyl–2,3–ethanediimine (2.0054 g, 5.3 mmol, 1 equiv.) in 61 mL ethyl acetate was charged with paraformaldehyde (0.1585 g, 5.3 mmol, 1 equiv.) and heated to 70 °C. Once heated, trimethylsilyl chloride was added (0.680 mL, 5.4 mmol, 1 equiv.) slowly darkening the yellow solution. After 2 hours a peach precipitate had formed, and the reaction was taken off heat to be placed in the freezer. After chilling overnight, the precipitate was collected over a glass frit and dried. Total yield: 1.9669 g, (94.3%).

^{1}H NMR (500 MHz, Chloroform–*d*) δ 10.13 (s, Hz, 1H), 8.15 (d, *J* = 1.6 Hz, 2H), 7.57 (t, *J* = 7.8 Hz, 2H), 7.35 (d, *J* = 7.9 Hz, 4H), 2.45 (sept, *J* = 6.8 Hz, 4H), 1.29 (d, *J* = 6.7 Hz, 12H), 1.25 (d, *J* = 6.9 Hz, 12H).

DCM at δ 4.11 and H_2O at δ 1.51.

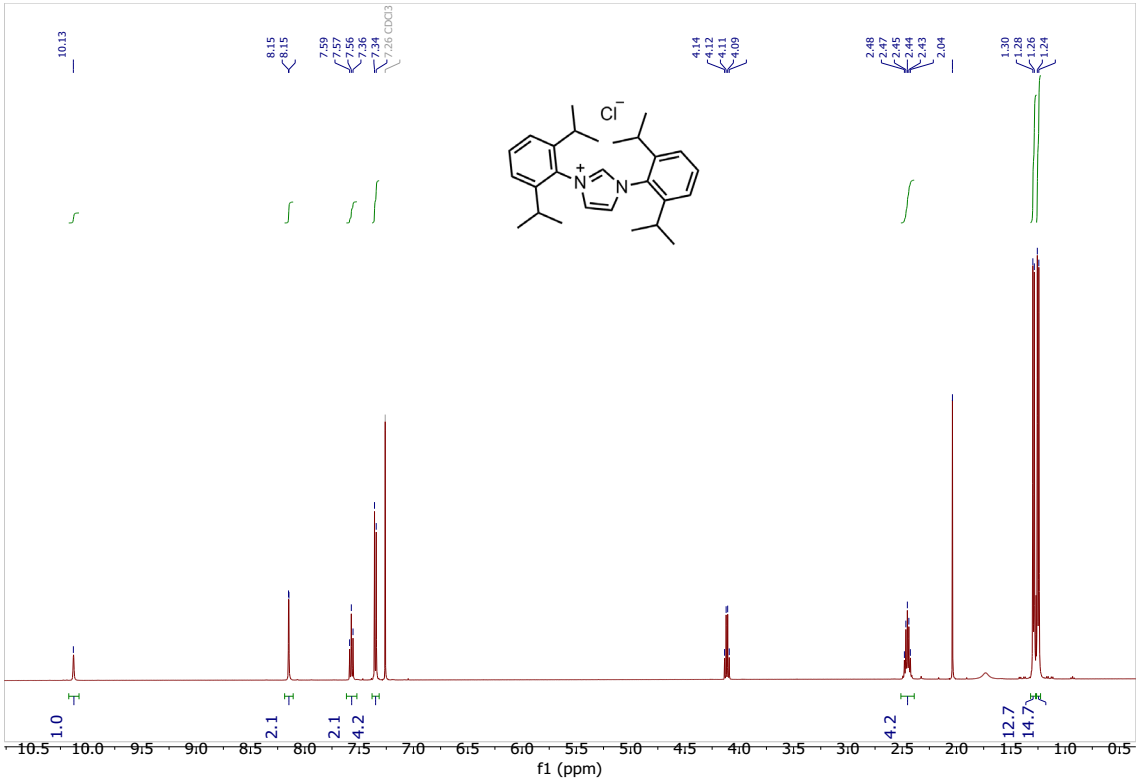

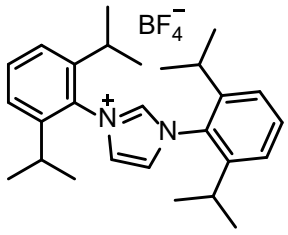

Synthesis of 1PTM – 55: 1,3–Bis(2,6–diisopropylphenyl)–imidazolium tetrafluoroborate: (1e) A solution of 1,3–Bis(2,6–diisopropylphenyl)–imidazolium chloride (0.9966 g, 2.52 mmol, 1 equiv.) in 25 mL of water was charged with a 50% (w/w) solution of HBF_4 (0.37 mL, 2.95 mmol, 1.1 equiv) dropwise. Upon addition, a

white precipitate immediately formed and upon full addition, the reaction stirred for 10 minutes. The reaction was extracted with DCM (3x10 mL) and dried using $MgSO_4$ then concentrated under vacuum until precipitate formed. Diethyl ether was used to precipitate a white solid that was collected over a glass frit and dried on a high vacuum line overnight. Total yield: 0.8674 g (72%).

^{1}H NMR (500 MHz, Chloroform–*d*) δ 8.70 (s, 1H), 7.83 (d, *J* = 1.7 Hz, 2H), 7.60 (t, *J* = 7.8 Hz, 2H), 7.37 (d, *J* = 7.8 Hz, 4H), 2.43 (sept, *J* = 6.8 Hz, 4H), 1.30 (d, *J* = 6.8 Hz, 12H), 1.22 (d, *J* = 6.9 Hz, 12H).

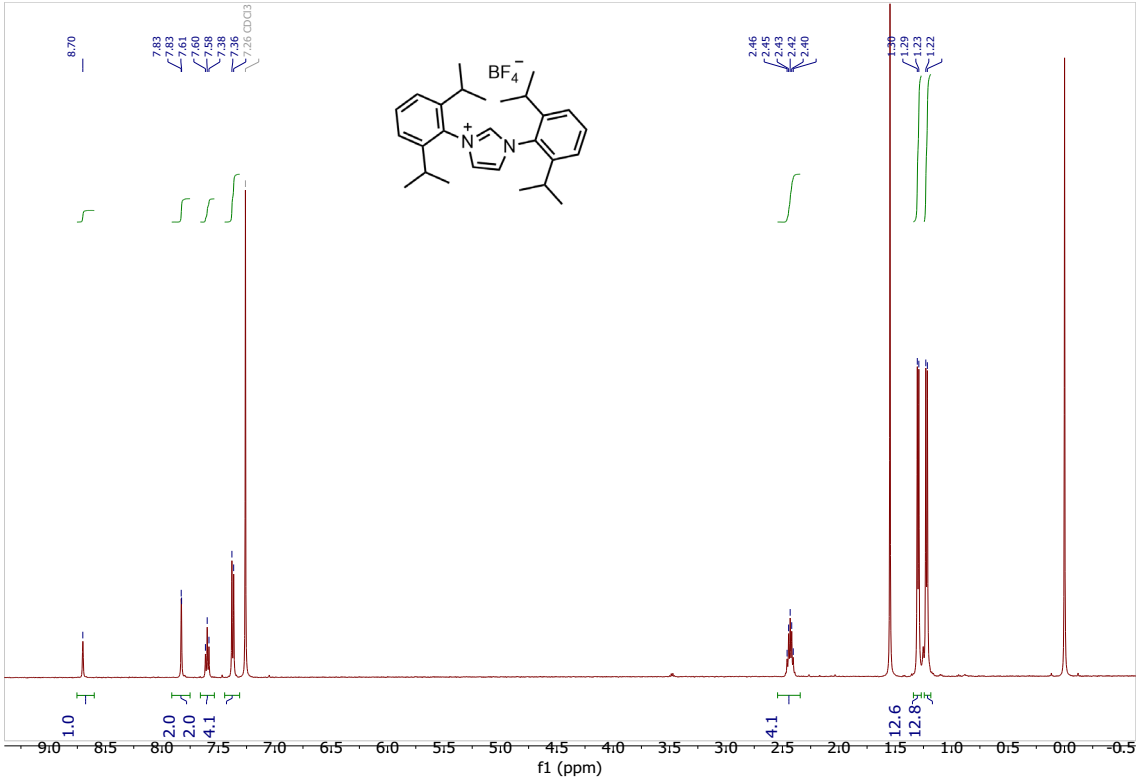

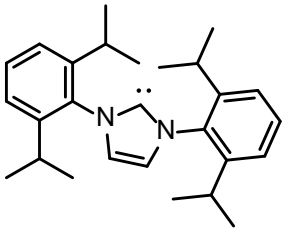

Synthesis of 1PTM – 59: 1,3–Bis(2,6–diisopropylphenyl)–imidazol–2–ylidene: (1d)

A solution of 1,3–Bis(2,6–diisopropylphenyl)–imidazolium tetrafluoroborate (0.8134 g, 1.71 mmol, 1 equiv.) and NaH (0.082 g, 3.42 mmol, 2 equiv.) in 10 mL of THF was charged with a small scoop (~0 g, 0 mmol, 0 equiv.). The reaction stirred at room temperature overnight and was filtered through a glass frit. The liquid phase was concentrated under vacuum leaving a pale gold precipitate. Total yield: 0.413 g, 62% yield).

^{1}H NMR (500 MHz, Benzene–d_6) δ 7.29 (t, 2H), 7.18 (d, J = 7.7 Hz, 4H), 6.61 (s, 2H), 2.96 (sept, J = 6.9 Hz, 4H), 1.28 (d, J = 6.9 Hz, 12H), 1.18 (d, J = 6.9 Hz, 12H).

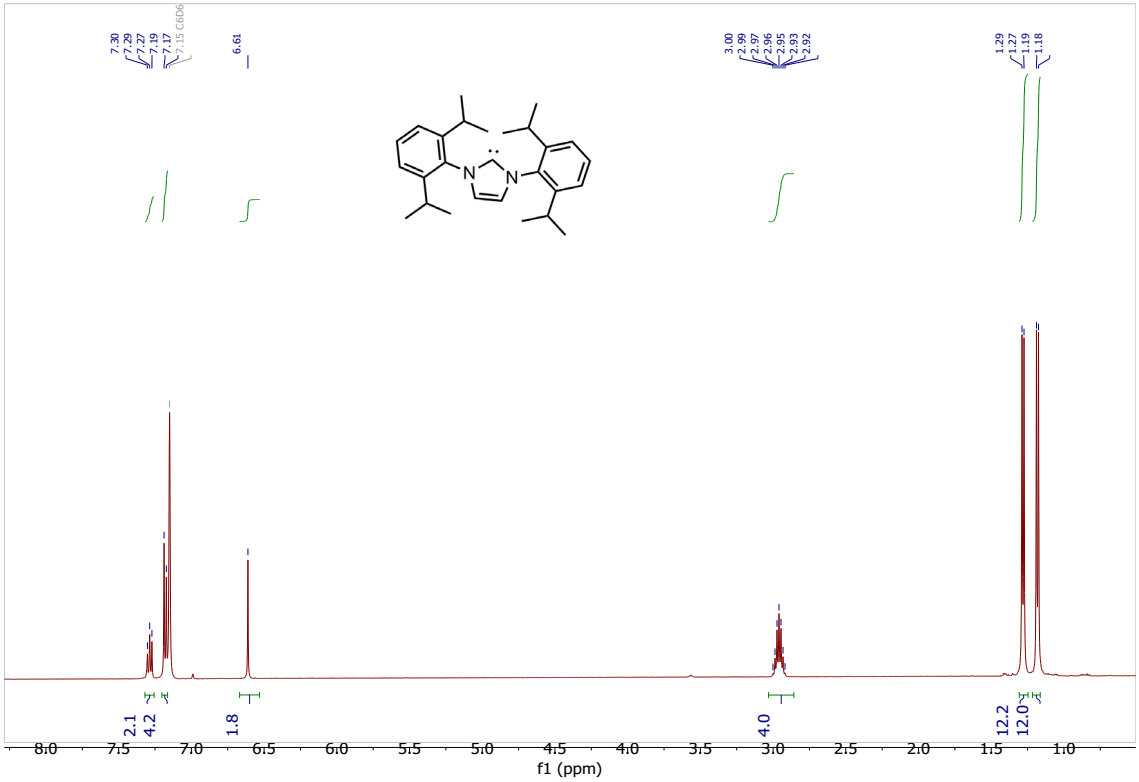

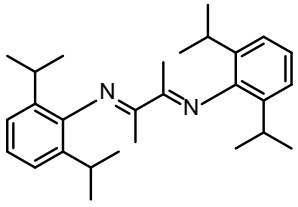

Synthesis of 1PTM – 81: N,N'–diisopropylphenyl–2,3–butanediimine: (4b) A solution of 2,6–diisopropylaniline (4.4 mL, 24.8 mmol, 2 equiv.) in 50 mL of methanol was heated to 50 °C and charged with acetic acid (0.3 mL, 5.3 mmol, 0 equiv.). To this solution, a second solution of 2,3–butanedione (1.1 mL, 12.8 mmol, 1 equiv.) in 24 mL of methanol was added slowly. Upon addition of 2,3–butanedione, the reaction yellowed and stirred overnight for 20 hr. After stirring, the reaction was concentrated under vacuum resulting in an orange oil. The oil was placed in a freezer with minimal methanol overnight yielding yellow crystals which were collected over a glass frit. Total yield: 3.211 g, (63.6%).

^{1}H NMR (500 MHz, Chloroform–*d*) δ 7.17 (d, *J* = 7.2 Hz, 4H), 7.10 (t, *J* = 6.8 Hz, 2H), 2.71 (sept, *J* = 6.9 Hz, 4H), 2.07 (s, 6H), 1.20 (d, *J* = 6.9 Hz, 12H), 1.18 (d, *J* = 6.8 Hz, 12H).

Methanol at δ 3.49, H_2O at δ 1.55

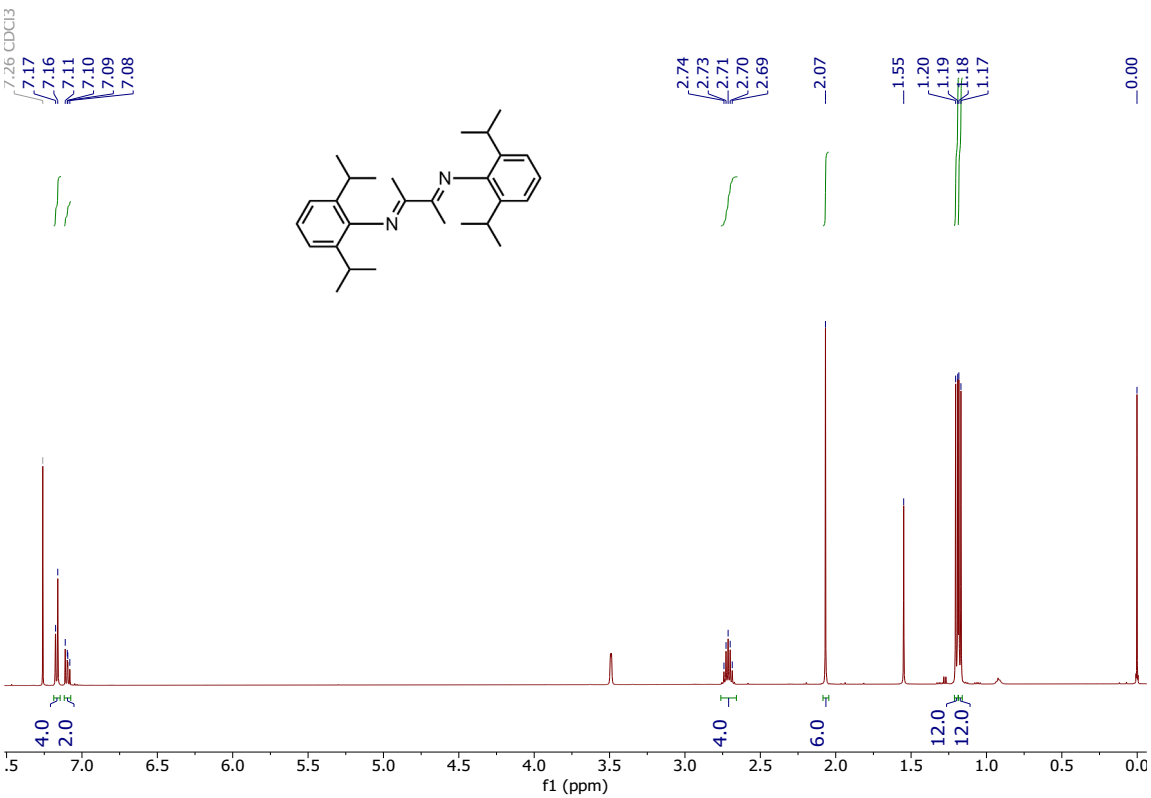

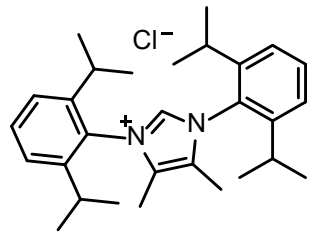

Synthesis of 1PTM – 106: [1,3–Bis(2,6–diisopropylphenyl)–4,5–dimethyl]imidazolium chloride: (4c) A solution of N,N'–diisopropylphenyl–2,3–butanediimine (0.6972 g, 1.71 mmol, 1 equiv.) in ethyl acetate was cooled to 0 °C in an ice bath. Separately, in a 10 mL scintillation vial, a solution of paraformaldehyde (0.0690 g, 2.23 mmol, 1.3 equiv.) was equilibrated in 4M HCl (0.68 mL, 2.72 mmol, 1.6 equiv.). After 10 minutes, the acidic solution was added to the diamine resulting in a reddening of the mixture. The reaction stirred overnight at room temperature. After stirring, the solution was a dark brown color and a beige precipitate had formed. The

precipitate was collected on a glass frit and washed with diethyl ether. Once dried, the solid was dissolved in minimal methanol and diethyl ether was used to precipitate out a white solid. Total yield: 0.4209 g, (54.3%).

^{1}H NMR (500 MHz, DMSO–d_6) δ 9.99 (s, 1H), 7.69 (t, J = 7.8 Hz, 2H), 7.55 (d, J = 7.8 Hz, 4H), 2.32 (sept, J = 6.8 Hz, 4H), 2.08 (s, 6H), 1.27 (d, J = 6.8 Hz, 12H), 1.12 (d, J = 6.8 Hz, 12H).

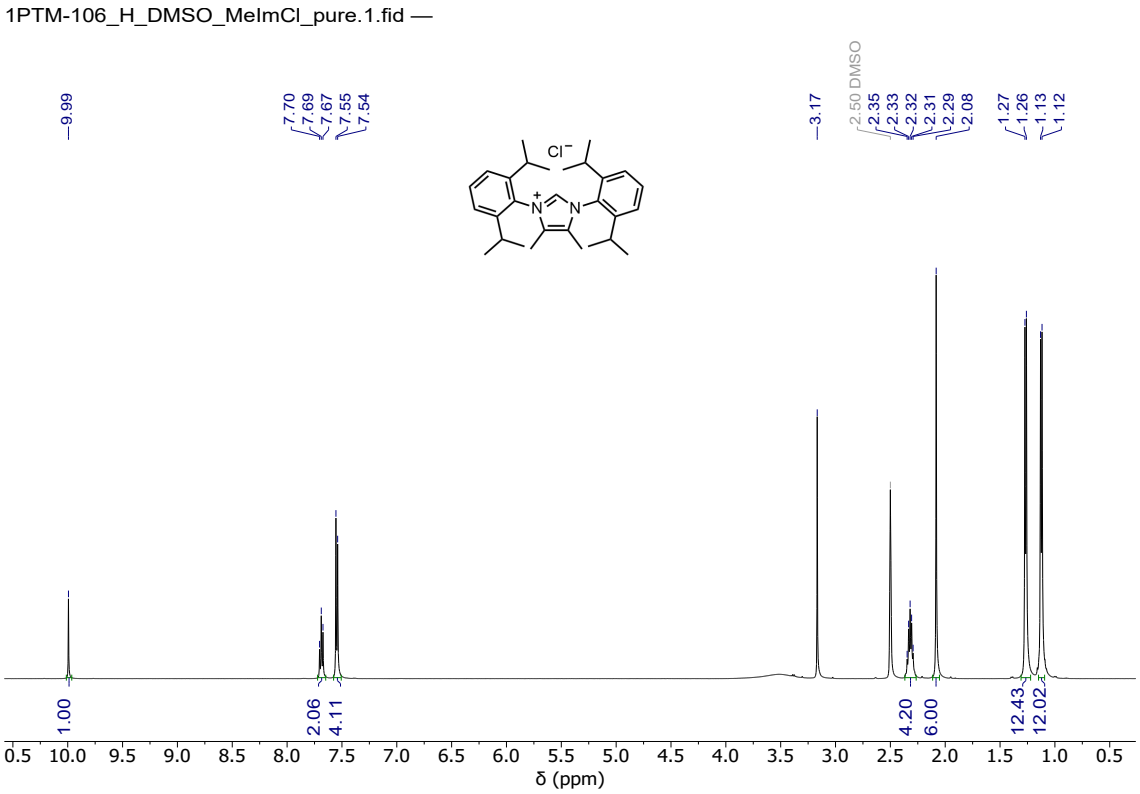

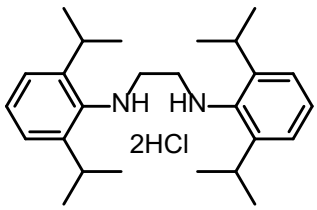

Synthesis of 1PTM – 93: N,N'–bis(2,6–diisopropylphenyl)ethylenediamine dihydrochloride: (2b) A solution of N,N'–diisopropylphenyl–2,3–ethanediimine (1.0015 g, 2.66 mmol, 1 equiv.) in THF was charged with $NaBH_4$ (0.4216 g, 11.1 mmol, 4 equiv.) and cooled to 0 °C. Once cool, concentrated HCl (36%) (0.46 mL, 5.32 mmol, 2 equiv.) was added dropwise over 20 minutes resulting in mild fizzing and the color to redden gently, then yellow finally resulting in a colorless solution once all the acid was added. The reaction was left to stir at 0 °C for 1 hour. After stirring, 3M dilute HCl (6 mL, excess) was added slowly. The resulting solution was allowed to slowly warm to room temperature and stirred overnight. After stirring, a white precipitate had formed. This was collected over a glass frit and washed with water. Total yield: 1.0031 g, (83.2%).

^{1}H NMR (500 MHz, DMSO–d_6) δ 7.24 (s, 6H), 3.38 (s, 4H), 3.37 – 3.32 (m, 4H), 1.17 (d, J = 6.7 Hz, 24H).

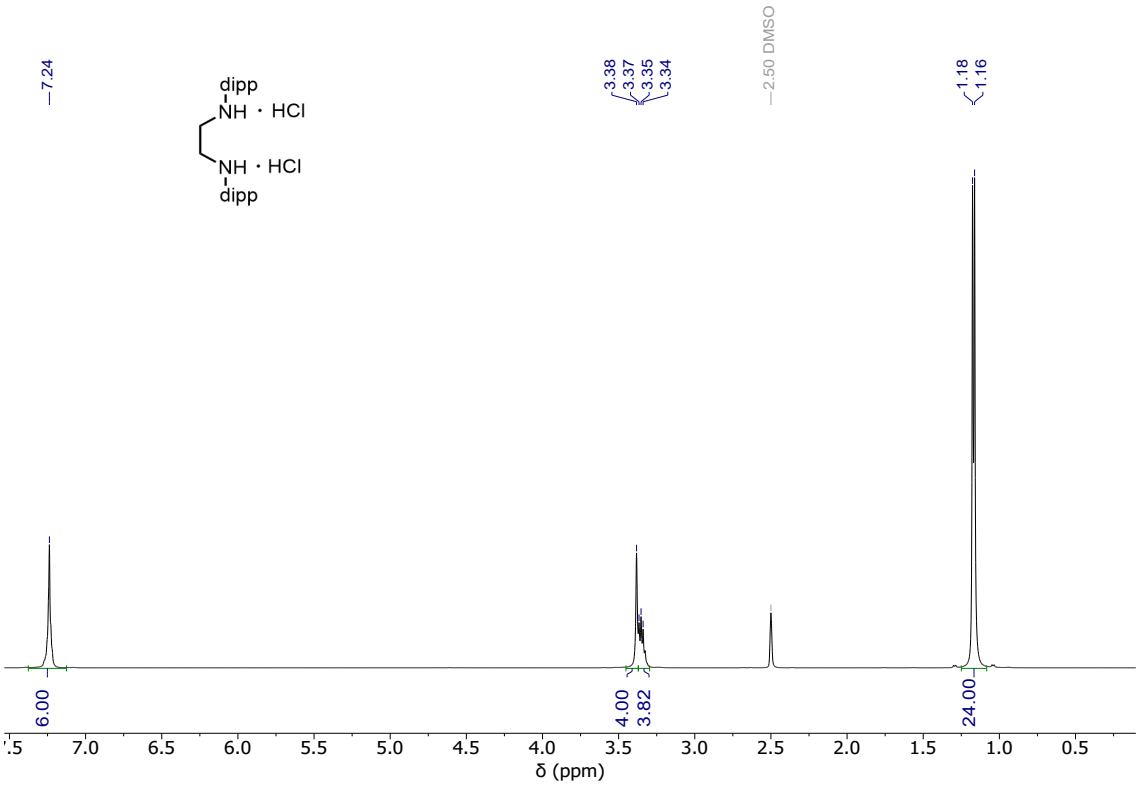

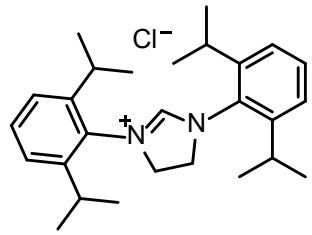

Synthesis of 2PTM – 005: 1,3–bis(2,6–diisopropylphenyl)imidazolinium chloride:

(2c) A solution of N,N'–bis(2,6–diisopropylphenyl)ethylenediamine dihydrochloride (0.750 g, 1.65 mmol, 1 equiv.) was made in triethyl orthoformate (6 mL, 36.1 mmol, excess) and heated to120 °C. Four drops of formic acid were added and a distillation setup was attached to catch evaporated ethanol. This solution stirred for 2 hours and approximately 2 mL of ethanol were collected. After stirring, heat was turned off and the reaction was left to cool slowly to r.t. and then stir overnight. A white precipitate

formed and was collected over a glass frit then washed with diethyl ether. Total yield: 0.701 g, (99%).

^{1}H NMR (500 MHz, DMSO–d_6) δ 9.45 (s, 1H), 7.55 (t, J = 7.8 Hz, 2H), 7.43 (d, J = 7.8 Hz, 4H), 4.53 (s, 4H), 3.08 (sept, 4H), 1.35 (d, J = 6.7 Hz, 12H), 1.19 (d, J = 6.8 Hz, 12H).

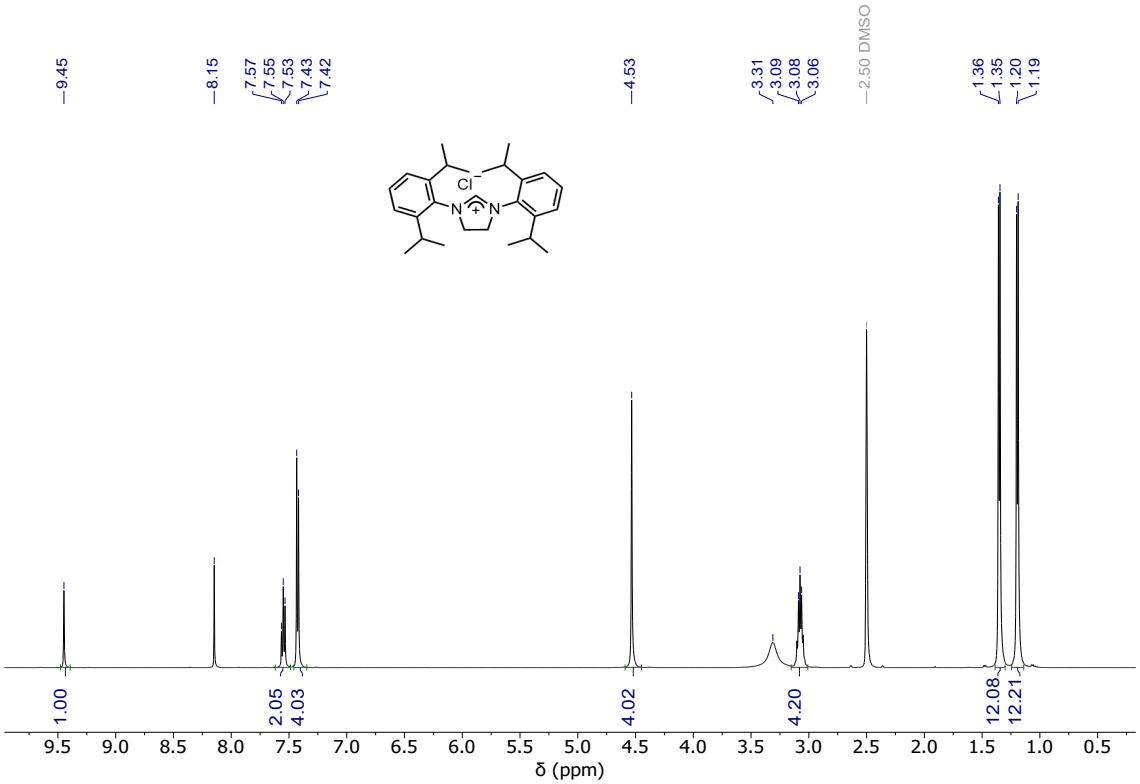

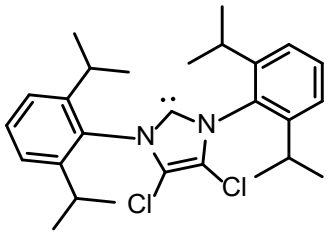

Synthesis of 1PTM – 75: 1,3–Bis(2,6–diisopropylphenyl)–4,5–dichloro–imidazol–2–ylidene: (3b) On a Schlenk line under inert N_2 atmosphere, a solution of 1,3–Bis(2,6–diisopropylphenyl)–imidazol–2–ylidene (1.0041 g, 2.57 mmol, 1 equiv.) in THF was

charged with CCl_4 (0.7 mL, 7.24 mmol, 2.8 equiv.). The reaction stirred overnight resulting in a brown solution which was dried under vacuum leaving a beige powder. Total yield: 0.9393 g, (79.9%).

^{1}H NMR (500 MHz, Benzene–d_6) δ 7.27 (t, J = 7.7 Hz, 2H), 7.15 (d, J = 5.9 Hz, 4H), 2.90 (sept, J = 6.9 Hz, 4H), 1.25 (d, J = 6.8 Hz, 12H), 1.21 (d, J = 6.9 Hz, 1H).

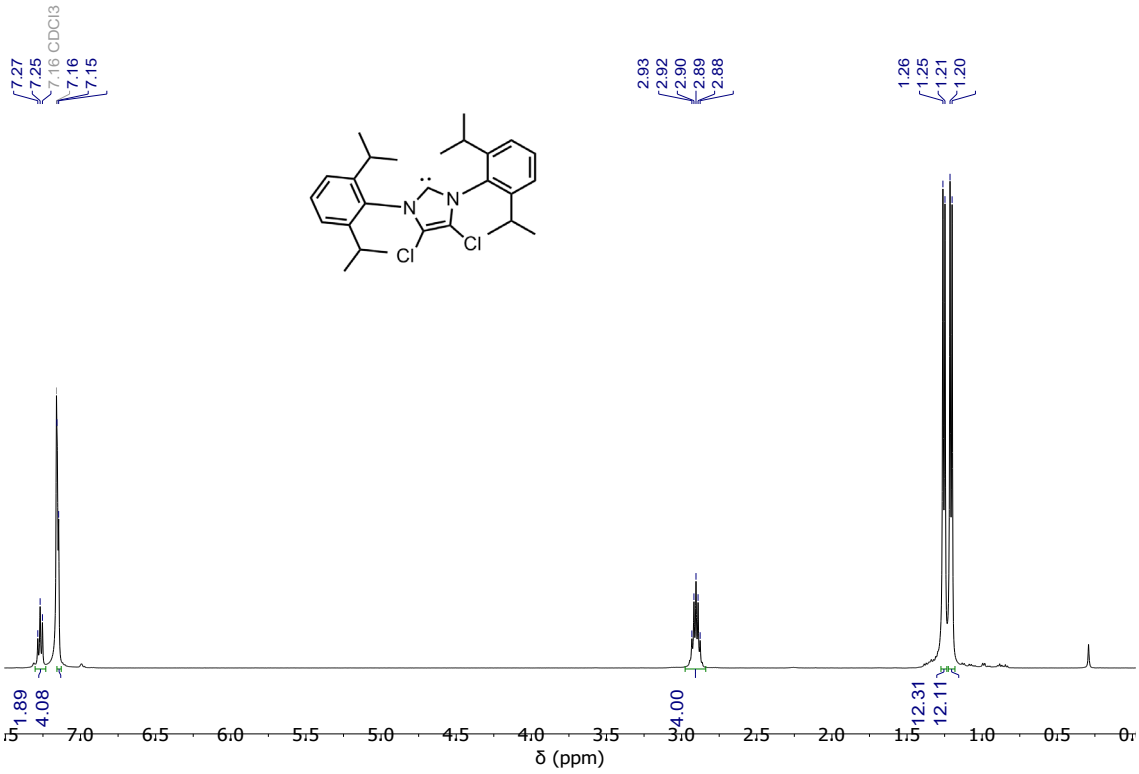

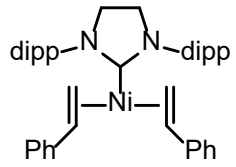

Synthesis of 3PTM – 001: (SIDipp)Ni(Sty)$_2$: (2a) In the N_2 glovebox a solution of 1,3–bis(2,6–diisopropylphenyl)imidazolinium chloride (0.2200 g, 0.514 mmol, 1 equiv.) in THF was charged with potassium tert–butoxide (0.0620 g, 0.550 mmol, 1

equiv.), and 60% (w/w) sodium hydride (0.0219 g, 0.548 mmol, 1 equiv.). This solution stirred at room temperature for 3 hours before being filtered through celite resulting in a light gold solution. In a separate scintillation vial, $Ni(COD)_2$ (0.1505 g, 0.547 mmol, 1 equiv.) was equilibrated with styrene (0.5 mL, 4.36 mmol, 8 equiv.) before being added in one pour to the NHC solution. The resulting red liquid stirred for 2 hours before solvent was removed over vacuum. The powder left behind was triturated in minimal THF and hexanes overnight in the freezer resulting in a dark green powder.

^{1}H NMR (500 MHz, Benzene–d_6) δ 7.27 (t, J = 7.7 Hz, 2H), 7.12 (d, J = 7.5, 4H), 6.97 (d, J = 8.2 Hz, 6H), 6.37 (d, J = 7.2 Hz, 4H), 3.63 – 3.5 (d, 4H), 3.53 – 3.38 (m, 4H), 3.15 (t, J = 11.2 Hz, 2H), 2.74 (dd, J = 28.2, 11.2 Hz, 4H), 1.44 (d, J = 6.7 Hz, 6H), 1.18 (d, J = 5.8 Hz, 6H), 1.11 (d, J = 6.9 Hz, 12H), 0.94 (d, J = 6.7 Hz, 6H).

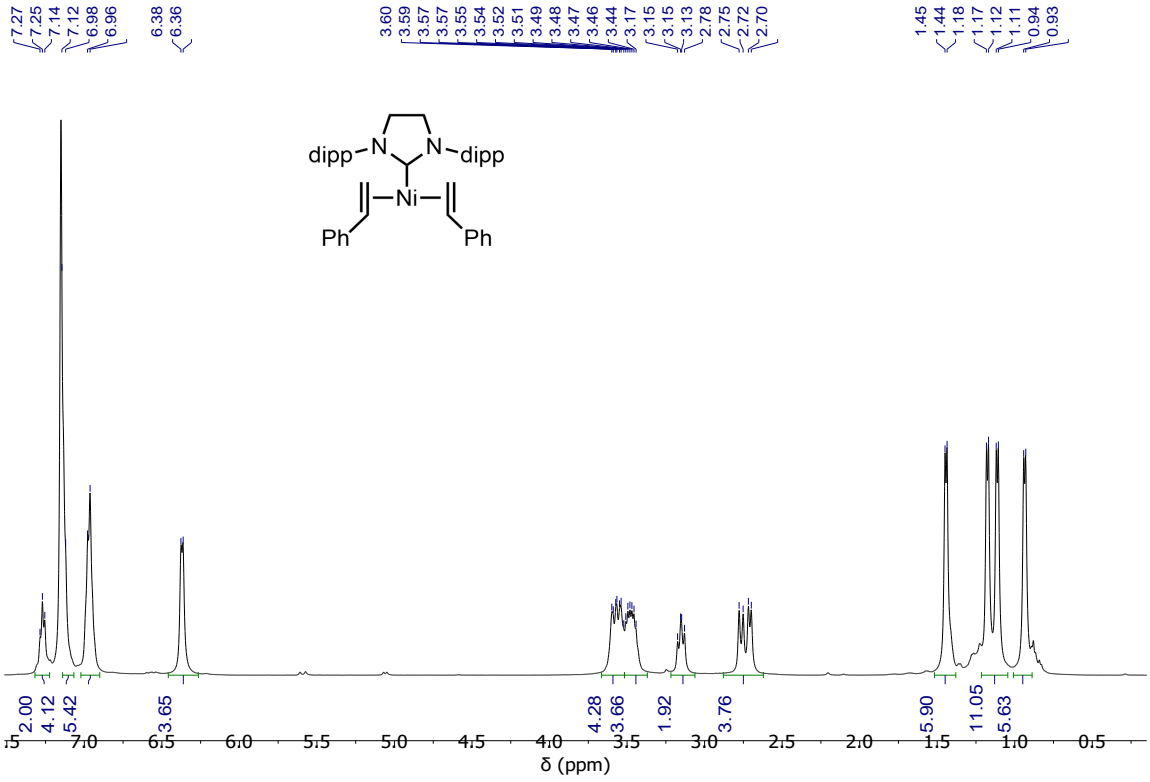

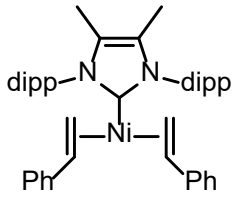

Synthesis of 3PTM – 002: (MeDipp)Ni(Sty)$_2$: (4a) In the N_2 glovebox a solution of [1,3–bis(2,6–diisopropylphenyl)–4,5–dimethyl]imidazolinium chloride (0.1650 g, 0.364 mmol, 1 equiv.) in THF was charged with potassium tert–butoxide (0.0433 g, 0.386 mmol, 1 equiv). This solution stirred at room temperature for 2 hours before being filtered through celite resulting in a light gold solution. In a separate scintillation vial, Ni(COD)$_2$ (0.1075 g, 0.0.391 mmol, 1 equiv.) was equilibrated with styrene (0.4 mL, 3.84 mmol, 8 equiv.) before being added in one pour to the NHC solution. The resulting red liquid stirred for 2 hours before solvent was removed over vacuum. The powder left behind was triturated in minimal THF and hexanes overnight in the freezer resulting in a dark yellow powder.

^{1}H NMR (500 MHz, Benzene–d_6) δ 7.32 (t, J = 7.7 Hz, 2H), 7.18 (d, J = 7.5 Hz, 4H), 7.00 (dd, J = 10.7, 6.9 Hz, 6H), 6.45 (d, J = 7.3 Hz, 4H), 3.38 (sept, J = 6.9 Hz, 2H), 3.22 (dd, J = 12.8, 9.3 Hz, 2H), 2.85 (sept, J = 6.7 Hz, 2H), 2.72 (dd, J = 19.4, 11.0 Hz, 4H), 1.65 (s, 6H), 1.42 (d, J = 6.7 Hz, 6H), 1.10 (d, J = 6.6 Hz, 6H), 0.98 (dd, J = 25.2, 6.9 Hz, 12H).

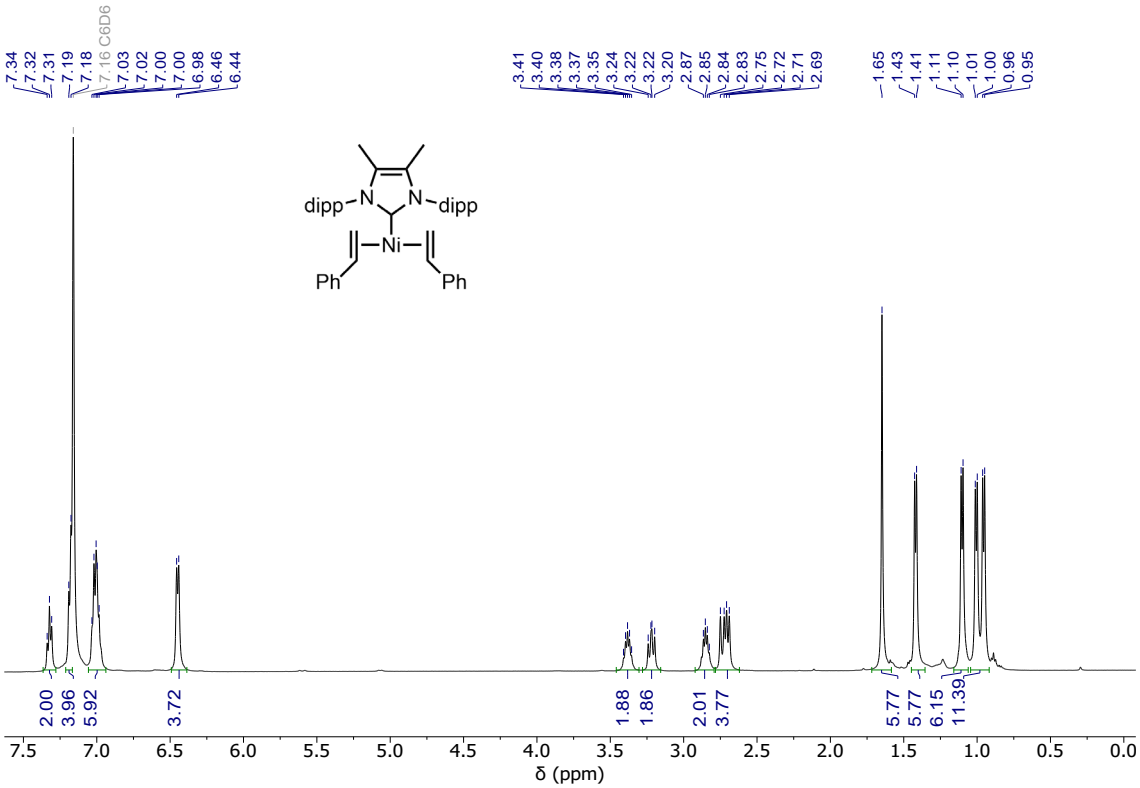

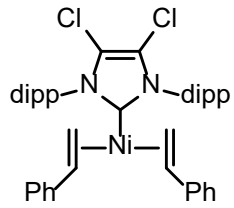

Synthesis of 3PTM – 001: (ClDipp)Ni(Sty)$_2$: (3a) In the N_2 glovebox a solution of 1,3–Bis(2,6–diisopropylphenyl)–4,5–dichloro–imidazol–2–ylidene () was made in THF. In a separate scintillation vial, Ni(COD)$_2$ (0.1515 g, 0.551 mmol, 1 equiv.) was equilibrated with styrene (0.5 mL, 4.36 mmol, 8 equiv.), for 15 minutes. This solution was added, in one pour, to the NHC solution resulting in a red liquid that stirred at room temperature for 2 hours. After stirring, the solution had darkened, and solvent was removed over vacuum. The resulting powder was triturated in minimal THF and hexanes overnight resulting in an orange crystal that was collected over a glass frit and dried on vacuum.

^{1}H NMR (500 MHz, Benzene–d_6) δ 7.30 (t, J = 7.8 Hz, 2H), 7.14 (d, J = 8.7 Hz, 4H), 6.97 (d, J = 2.4 Hz, 6H), 6.45 – 6.33 (m, 4H), 3.34 (sept, J = 6.8 Hz, 2H), 3.23 (dd, J = 12.9, 9.3 Hz, 2H), 2.86 (sept, J = 6.7 Hz, 2H), 2.77 (dd, J = 27.2, 11.1 Hz, 4H), 1.39 (d, J = 6.7 Hz, 6H), 1.06 (d, J = 6.9 Hz, 6H), 0.98 (d, J = 6.9 Hz, 6H).

Hexanes at δ 1.25, 0.89

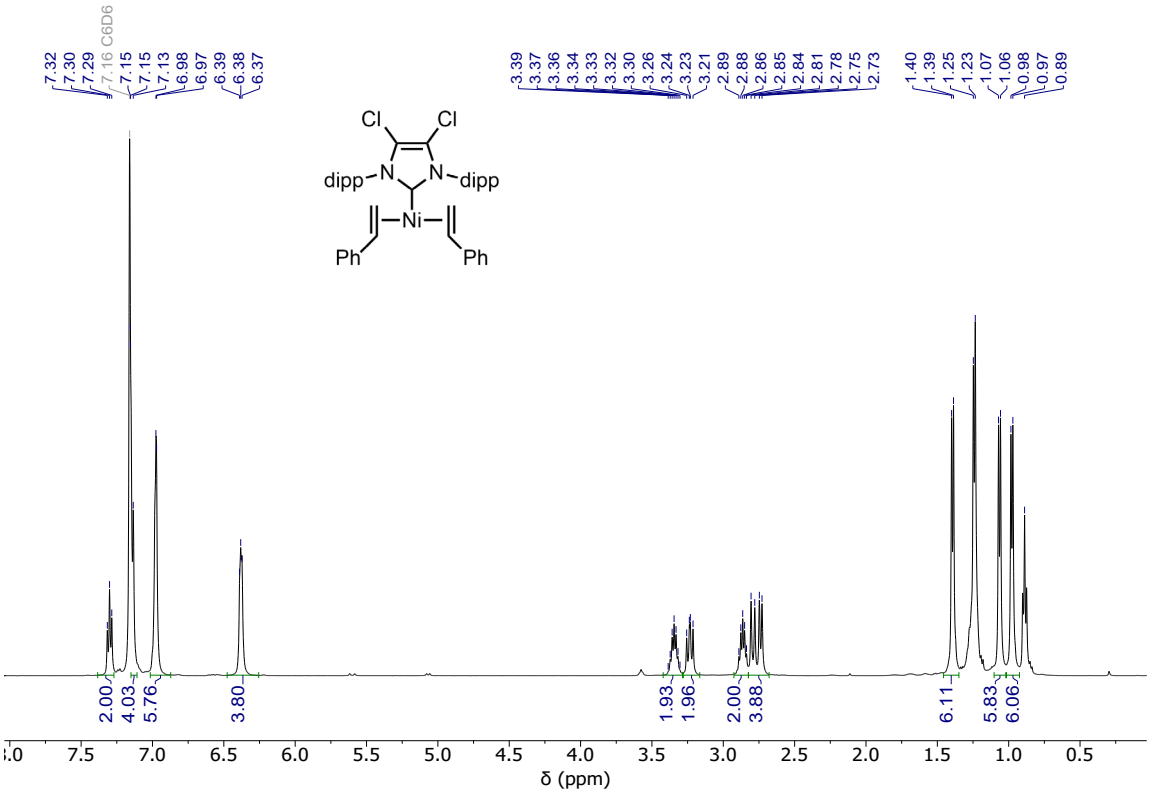

Bibliography

1. Hassam, M.; Taher, A.; Arnott, G. E.; Green, I. R.; van Otterlo, W. A. L. Isomerization of Allylbenzenes. *Chem. Rev.* **2015**, *115* (11), 5462–5569.
2. Kapat, A.; Sperger, T.; Guven, S.; Schoenebeck, F., Olefins through Intramolecular Radical Relocation. Science 2019, 363 (6425), 391. https://doi.org/10.1126/science.aav1610.
3. Troegel, D.; Stohrer, J. Recent Advances and Actual Challenges in Late Transition Metal Catalyzed Hydrosilylation of Olefins from an Industrial Point of View. *Coordination Chemistry Reviews* **2011**, *255* (13), 1440–1459. https://doi.org/10.1016/j.ccr.2010.12.025.
4. Nakajima, Y.; Shimada, S. Hydrosilylation Reaction of Olefins: Recent Advances and Perspectives. *RSC Adv.* **2015**, *5* (26), 20603–20616. https://doi.org/10.1039/C4RA17281G.
5. Afon'kin, I. S.; Sotnikov, A. M.; Gataullin, R. R.; Spirikhin, L. V.; Abdrakhmanov, I. B. Reactions of N– and C–Alkenylanilines: Vi. Synthesis of 6–Methyl–2–[(E or Z)–1–Propenyl]Anilines and the Corresponding Anilides and Their Reaction with Bromine. Russ. J. Org. Chem. 2004, 40, 1764−1768.
6. Scarso, A.; Colladon, M.; Sgarbossa, P.; Santo, C.; Michelin, R. A.; Strukul, G. Highly Active and Selective Platinum(II)–Catalyzed Isomerization of Allylbenzenes: Efficient Access to (E)–Anethole and Other Fragrances via Unusual Agostic Intermediates. *Organometallics* **2010**, *29* (6), 1487–1497.
7. Spallek, M. J.; Stockinger, S.; Goddard, R.; Trapp, O. "Modular palladium bipyrazoles for the isomerization of allylbenzenes – mechanistic considerations and insights into catalyst design and activity, role of solvent, and additive effects." *Adv. Synth. Catal.* **2012**, *354*, 1466–1480.
8. Wang, Y.; Qin, C.; Jia, X.; Leng, X.; Huang, Z. An Agostic Iridium Pincer Complex as a Highly Efficient and Selective Catalyst for Monoisomerization of 1–Alkenes to Trans–2–Alkenes. *Angew. Chemie – Int. Ed.* **2017**, *56* (6), 1614–1618. https://doi.org/10.1002/anie.201611007.
9. Crossley, S. W. M.; Barabé, F.; Shenvi, R. A. Simple, Chemoselective, Catalytic Olefin Isomerization. *J. Am. Chem. Soc.* **2014**, *136* (48), 16788–16791. https://doi.org/10.1021/ja5105602.
10. Schmidt, A.; Nödling, A. R.; Hilt, G. "An Alternative Mechanism for the Cobalt–Catalyzed Isomerization of Terminal Alkenes to (Z)–2–Alkenes." Angew. Chem. Int. Ed. 2015, 54, 801–804. https://onlinelibrary.wiley.com/doi/full/10.1002/anie.201409902
11. Kiso, Y.; Kumada, M.; Tamao, K.; Umeno, M. Silicon Hydrides and Nickel Complexes: I. Phosphine–Nickel(II) Complexes as Hydrosilylation Catalysts. *Journal of Organometallic Chemistry* **1973**, *50* (1), 297–310. https://doi.org/10.1016/S0022–328X(00)95116–7.
12. Biswas, S. Mechanistic Understanding of Transition–Metal–Catalyzed Olefin Isomerization, *Comments on Inorganic Chemistry* **2015**, *35* (6), 300–330. https://doi.org/10.1080/02603594.2015.1059325.

13. Tolman, C. A. Chemistry of Tetrakis (Triethyl Phosphite)–Mechanism of Olefin Isomerization. *Journal of the American Chemical Society* **1972**, *94* (9), 2994–2999.
14. Bartlett, S. A.; Badiola, K. A.; Arandiyan, H.; Masters, A. F.; Maschmeyer, T. The Autocatalytic Isomerization of Allylbenzene by Nickel(0) Tetrakis(Triethylphosphite). *European Journal of Inorganic Chemistry* **2018**, *2018* (29), 3384–3387.
15. Jennerjahn, R.; Jackstell, R.; Piras, I.; Franke, R.; Jiao, H.; Bauer, M.; Beller, M. Benign Catalysis with Iron: Unique Selectivity in Catalytic Isomerization Reactions of Olefins. ChemSusChem 2012, 5, 734−739.
16. Pappas, I.; Treacy, S.; Chirik, P. J. Alkene Hydrosilylation Using Tertiary Silanes with α–Diimine Nickel Catalysts. Redox–Active Ligands Promote a Distinct Mechanistic Pathway from Platinum Catalysts. ACS Catal. 2016, 6 (7), 4105–4109. https://doi.org/10.1021/acscatal.6b01134.
17. Felten, S.; Marshall, S. F.; Groom, A. J.; Vanderlinden, R. T.; Stolley, R. M.; Louie, J. Synthesis and Characterization of [(NHC)Ni(Styrene)2] Complexes: Isolation of Monocarbene Nickel Complexes and Benchmarking of %VBur in (NHC)Ni–π Systems. Organometallics 2018, 37 (21), 3687–3697.
18. Liu, H.; Xu, M.; Cai, C.; Chen, J.; Gu, Y.; Xia, Y. Cobalt–Catalyzed Z to E Isomerization of Alkenes: An Approach to €–β–Substituted Styrenes. *Org. Lett.* **2020**, *22* (3), 1193–1198.
19. Bantreil, X.; Nolan, S. P. Synthesis of N–Heterocyclic Carbene Ligands and Derived Ruthenium Olefin Metathesis Catalysts. *Nature Protocols* **2011**, *6* (1), 69–77. https://doi.org/10.1038/nprot.2010.177
20. Arduengo, A., Dias, R., Harlow, R.L., Kline, M J. Am. Chem. Soc. (1992), 114, 5530–5534
21. Arduengo, A., Krafczyk, R., Schmutzler, R., Tetrahedron, (1999), 55, 14523–14534
22. Beillard, A.; Métro, T.–X.; Bantreil, X.; Martinez, J.; Lamaty, F. Cu(0), O2 and Mechanical Forces: A Saving Combination for Efficient Production of Cu–NHC Complexes. *Chem. Sci.* **2017**, *8* (2), 1086–1089. https://doi.org/10.1039/C6SC03182J
23. Hans, M.; Lorkowski, J.; Demonceau, A.; Delaude, L. Efficient Synthetic Protocols for the Preparation of Common N–Heterocyclic Carbene Precursors. *Beilstein Journal of Organic Chemistry* **2015**, *11*, 2318–2325. https://doi.org/10.3762/bjoc.11.252.
24. Zeng, W.; Wang, E.; Qiu, R.; Sohail, M.; Wu, S.; Chen, F.–X. Oxygen–Atom Insertion of NHC–Copper Complex: The Source of Oxygen from N,N–Dimethylformamide. *Journal of Organometallic Chemistry* **2013**, *743*, 44–48. https://doi.org/10.1016/j.jorganchem.2013.06.017.